ACS APPLIED MATERIALS & INTERFACES

Review

www.acsami.org

Cell Response to Nanocrystallized Metallic Substrates Obtained through Severe Plastic Deformation

Sara Bagherifard,*[,†,‡,§,∥] Ramin Ghelichi,[†,⊥] Ali Khademhosseini,*[,‡,§,#,∇,○] and Mario Guagliano[†]

[†]Department of Mechanical Engineering, Politecnico di Milano, Via G. La Masa, 1, 20156, Milan, Italy

[‡]Harvard-MIT Division of Health Sciences and Technology, Massachusetts Institute of Technology (MIT), Cambridge, Massachusetts 02139, United States

[§]Center for Biomedical Engineering, Department of Medicine, Brigham and Women's Hospital, Harvard Medical School, Boston, Massachusetts 02139, United States

[∥]David H. Koch Institute for Integrative Cancer Research, Massachusetts Institute of Technology (MIT), Cambridge, Massachusetts 02139, United States

[⊥]Department of Mechanical Engineering, Massachusetts Institute of Technology (MIT), Cambridge, Massachusetts 02139, United States

[#]Wyss Institute for Biologically Inspired Engineering, Harvard University, Boston, Massachusetts 02115, United States

[∇]Department of Maxillofacial Biomedical Engineering and Institute of Oral Biology, School of Dentistry, Kyung Hee University, Seoul, 130-701, Republic of Korea

[○]Department of Physics, King Abdulaziz University, Jeddah, 21569, Saudi Arabia

ABSTRACT: Cell−substrate interface is known to control the cell response and subsequent cell functions. Among the various biophysical signals, grain structure, which indicates the repeating arrangement of atoms in the material, has also proved to play a role of significant importance in mediating the cell activities. Moreover, refining the grain size through severe plastic deformation is known to provide the processed material with novel mechanical properties. The potential application of such advanced materials as biomedical implants has recently been evaluated by investigating the effect of different substrate grain sizes on a wide variety of cell activities. In this review, recent advances in biomedical applications of severe plastic deformation techniques are highlighted with special attention to the effect of the obtained nano/ultra-fine-grain size on cell−substrate interactions. Various severe plastic deformation techniques used for this purpose are discussed presenting a brief description of the mechanism for each process. The results obtained for each treatment on cell morphology, adhesion, proliferation, and differentiation, as well as the in vivo studies, are discussed. Finally, the advantages and challenges regarding the application of these techniques to produce multifunctional bio-implant materials are addressed.

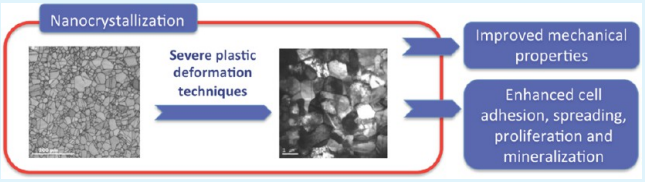

KEYWORDS: *nanocrystallization, severe plastic deformation, cell−substrate interaction, cellular activity, grain size, biocompatibility*

INTRODUCTION

Superior mechanical properties are indispensable prerequisite of biomaterials that are predominantly used in mechanically loaded areas to stabilize and promote the integrity of fractures, replace joints, and realign bone fragments. In addition to mechanical stability under physiological strains and stresses, the implant materials should provide the biological potential to support the healing process. There are various biophysical parameters interfering with the functionality of biomaterials in such applications, among which surface characteristics as microstructure and topography are proved to play a key role.

A large body of knowledge has been provided by previous studies on the effects of surface topography on cellular function at the cell substrate interface. Cell adhesion, morphology, proliferation, migration, and differentiation have been studied in a wide variety of cell types ranging from fibroblasts to mesenchymal stem cells (MSCs).[1−16] The topographical features are also reported to reduce the formation of biofilms that are resistant to antimicrobial agents and consequently decrease the risk of infections in many applications.[13,17−22]

Crystal structure can be also considered as a key factor influencing almost all characteristics of polycrystalline materials. It is generally defined as the arrangement of atoms or molecules in the solid state, in a pattern that is repetitive in all spatial dimensions. This periodic array, known also as crystallite or grain, can include vacancies (point defects) and dislocations (linear defects) in the idealized atomic/molecular arrangement. These defects contribute to the mechanical properties of

Received: February 23, 2014
Accepted: April 22, 2014
Published: April 22, 2014

material. Almost all metals are polycrystalline that is they have a structure composed of crystals with varying size and orientations. Where the individual crystals/grains meet is called grain boundary.[23]

In the recent years, the role of crystal size in altering the material biological characteristics has been studied on different ranges of material. Indeed nanograined (NG) surfaces are considered to have the potential to alter absorption of proteins that mediate cell adhesion and control and enhance subsequent cell functions and tissue growth.[24] Relative increase in surface area and enhanced reactivity are the distinctive intrinsic aspects of NG materials giving them the potential to manipulate their interaction with cells.

It is well recognized that severe plastic deformation (SPD) can result in extreme grain refinement obtaining ultra-fine-grained (UFG) material through large deformations applied at high strain rates and relatively low temperatures.[25−27] The engineering definition of SPD methods provided by Valiev et al.,[25] describes such methods as any metal forming process that imposes high strain rates without significantly changing the overall dimensions of the bulk material; such methods are known to result in exceptional grain refinement. UFG solids, on the other hand, are described specifically as bulk solids having fairly homogeneous structures with average crystal sizes smaller than ∼1 μm.[25,28] The structure of the SPD material is characterized by the formation of UFG as well as the presence of grain boundaries with high density of dislocations and vacancies, numerous lattice distortions, and possible phase composition alteration.[25] The permanent storage of dislocations in boundaries with increasing deformation leads to an increase of the misorientations.[27]

Originally, NG materials were obtained through the combination of nanofabrication methods involving powder metallurgy,[29] chemistry and heat treatment,[30,31] and sintering.[32,33] Majority of these methods result in residual porosities, impurities, and evoke dimensional issues. Being able to eliminate the aforementioned concerns, SPD techniques are recognized as practical alternatives of conventional thermo mechanical methods for obtaining UFG/NG material, boosting the application of NG material in many different fields.[34] Besides, SPD approaches can produce material with relatively higher strength and novel mechanical properties.[25,35] This particular combination has not been provided by other traditional techniques.

Being established on the fundamental principles of metal forming, which date back to 2000 years ago,[28] the first practical developments of NG materials generated through SPD were reported in 1991;[36] since then many of such methods have been developed to produce bulk or surface NG materials with unparalleled physical and mechanical properties. The UFG materials obtained through SPD methods have been studied mainly for their superior mechanical characteristics compared to their microcrystalline counterparts. There are many publications on production and characterization of a wide range of UFG/NG metals and alloys produced by SPD methods, studying the grain refinement mechanism as well as their enhanced yield strength, improved fatigue behavior, hardness, corrosion, wear, friction and scratch resistance, thermal stability, magnetic properties, and chemical reactions.[37−51]

It has been recently shown that SPD methods can provide bulk/surface materials with advanced multifunctional properties that make them beneficial for biomedical applications.[26] Exceptional mechanical characteristics promote the functionality of the SPD material under physiological strains, offering the possibility to avoid the use of expensive and potentially toxic or allergenic elements and providing the opportunity of downsizing the implant and medical device and possibly reducing the surgical intervention's consequences. For example, Ti alloys particularly Ti6Al4V are commonly used for implants due to their outstanding mechanical characteristics; this alloy is lightweight, corrosion resistant, and has a high degree of biocompatibility. Nevertheless, it contains the toxic ions of Al and V, the risk of extraction of which into body fluids over time is a serious concern.[52] SPD can provide the solution to this problem by increasing the strength of pure Ti making it comparable to that of Ti6Al4V.[53]

In the past few years, there has been a breakthrough in studying the potential applications of SPD-based technologies in biomedical field, focusing on the effect of UFG/NG on cell/bacteria response. Previous studies on NG material, produced mostly through powder compacting methods, have provided indications on the effect of NG substrates on manipulating cell behavior through cell substrate interactions. Webster et al. provided the first evidence of enhanced osteoblast attachment and function on NG ceramics (alumina, titania, and hydroxyapatite (HA))[32,33,54,55] and later on NG metals (Ti, Ti6Al4V, and CoCrMo alloys).[29,56,57] Balasundaram and Webster[56] suggested NG materials as a new option for orthopedic implants due to their ability to simulate the dimensions of the constituents and components of natural bone-like proteins and HA. The increased cell adhesion was reported to be due to higher percentages of grain boundaries on the surface of NG material considering that osteoblasts adhere specifically at grain boundaries.[29] It is to be mentioned that the NG and CG samples used in the latter studies, all obtained through powder metallurgy process, had a porosity of 5−10% and represented different surface nanotopographies. Therefore, it is difficult to attribute the reported observations directly to the grain size effect. Biocompatibility improvement was also reported for Ti subjected to plasma treatment that not only refined the surface grains to nanosize but also altered the surface roughness and surface chemical composition, thus again impeding to perform an independent study solely on the effect of grain size.[58]

SPD treated materials are also reported to provide the possibility of controlling the cell behavior in contact with the UFG/NG structure. There are reports of their improved biocorrosion behavior and effect on decreasing bacterial adhesion and biofilm formation. All in all these techniques are able to provide the implant with a combination of specific mechanical properties, microstructure, topography, and biological characteristics, which can optimize mechanical functionality as well as biocompatibility.[59] The latter characteristics have made the application of these techniques in biomedical field, a vigorously growing area of research with promising technical and biological benefits.

There are a series of parameters studied to affect the cell response to different bioimplant materials, among which wettability has been recognized as a key parameter. Degree of wettability known also as hydrophilicity is correlated with the ability of the solid surface to reduce the surface tension of the liquid phase in contact with it.[60] To assess the wettability characteristics of a surface, the contact angle of the liquid is measured in the interface. Small contact angles ($\ll 90°$) correspond to high wettability, while large contact angles

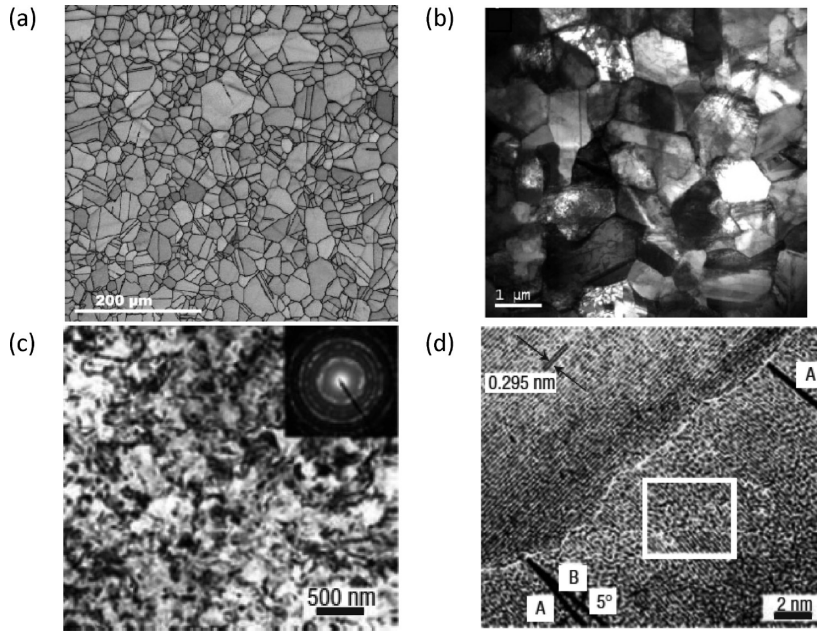

Figure 1. (a) Scanning electron micrograph of as-received austenitic stainless steel; (b) transmission electron micrograph of the same material subjected to SPD treatment; (c) transmission electron micrograph of titanium after SPD (with the selected area diffraction pattern as an inset); (d) high resolution electron micrograph representing high distortion in crystal lattice and variation of disorientation in the same material as (c),[62,63] adapted with permission from John Wiley & Sons and Nature Publishing Group.

($\gg$90°) correspond to low wettability. Surface topography and grain size are among the most important parameters that affect the wettability of a surface. While in terms of surface roughness effect on cell substrate interface, collectively the studies imply improved cell behavior,[15] in case of grain size effect less straightforward data is available.

In this review, the recent advances in biomedical applications of SPD techniques are highlighted with special attention to the effect of the obtained NG/UFG grain size on cell−substrate interaction. Various SPD techniques used for this purpose are discussed presenting a brief description of the mechanism for each process. The results obtained on cell adhesion, morphology, proliferation, and differentiation as well as in vivo studies are discussed. In the end the advantages and challenges regarding application of these techniques for producing multifunctional biomaterials are addressed.

2. SPD TECHNIQUES

Grain refinement occurs through the formation and rearrangement (annihilation and recombination) of lattice defects to create grain boundaries separating individual crystals.[61] Numerous models have been suggested to describe the mechanism of grain refinement via SPD. However, the basic concept of the most commonly accepted ones is that the continual reduction in the average grain size occurs as a consequence of interaction of dislocations in the plastically deformed crystals.[47]

Different microscopical techniques have been applied to characterize the grain size refinement generated through SPD. Figure 1 represents the (a) scanning electron micrograph of as-received austenitic stainless steel evidenced through surface polishing and subsequent acid etching (average grain size of 22 μm) and (b) the transmission electron micrograph of the same material subjected to SPD treatment. The grain refinement effect of the applied SPD approach is clearly observed in this figure.[62] SPD processed titanium observations by transmission electron microscopy and high-resolution electron microscopy, as shown in Figure 1c and d, respectively, similarly reveal the NG structure obtained after the SPD process showing highly distorted grain boundaries. The curvilinear grain boundaries in Figure 1d represent the presence of numerous atomic defects as well as the variation in the misorientation angle along the same boundary by about 5° which can indicate the presence of disclinations.

Since the first evidences of grain refinement through SPD, there has been an evolution in the developed approaches and a quite vast range of methods have been developed. In this study, we have mainly focused on the approaches that have been used in biomedical fields. A comprehensive review on a wide variety of SPD methods for general industrial applications can be found in ref 47.

2.1. Equal Channel Angular Pressing. Equal channel angular pressing (ECAP) process is among the most widely used SPD techniques adopted for producing UFG materials in bulk. In this technique, the billet sample is pressed through a die consisting of two intersecting channels with identical profiles meeting at an angle of ϕ in the inner corner and an angle of α in the outer one.[63,64] The channels normally intersect at an angle of 90°; however, alternative options of $\phi >$ 90° are also considered. The mechanism of ECAP is schematically illustrated in Figure 2a.

The high plastic deformation induced through repeated passes result in extreme and uniform grain refinement without changing the cross section of the billet. Grain refinement is relatively easy to obtain by ECAP; however, in order to obtain extreme grain refinement, number of passes, sequence of orientations of the billets relative to the die as well as other process features should be optimized.[63] The final size of the grains depends strongly on the material and processing parameters. Still the typical grain size range reported for ECAP material is 200−300 nm.

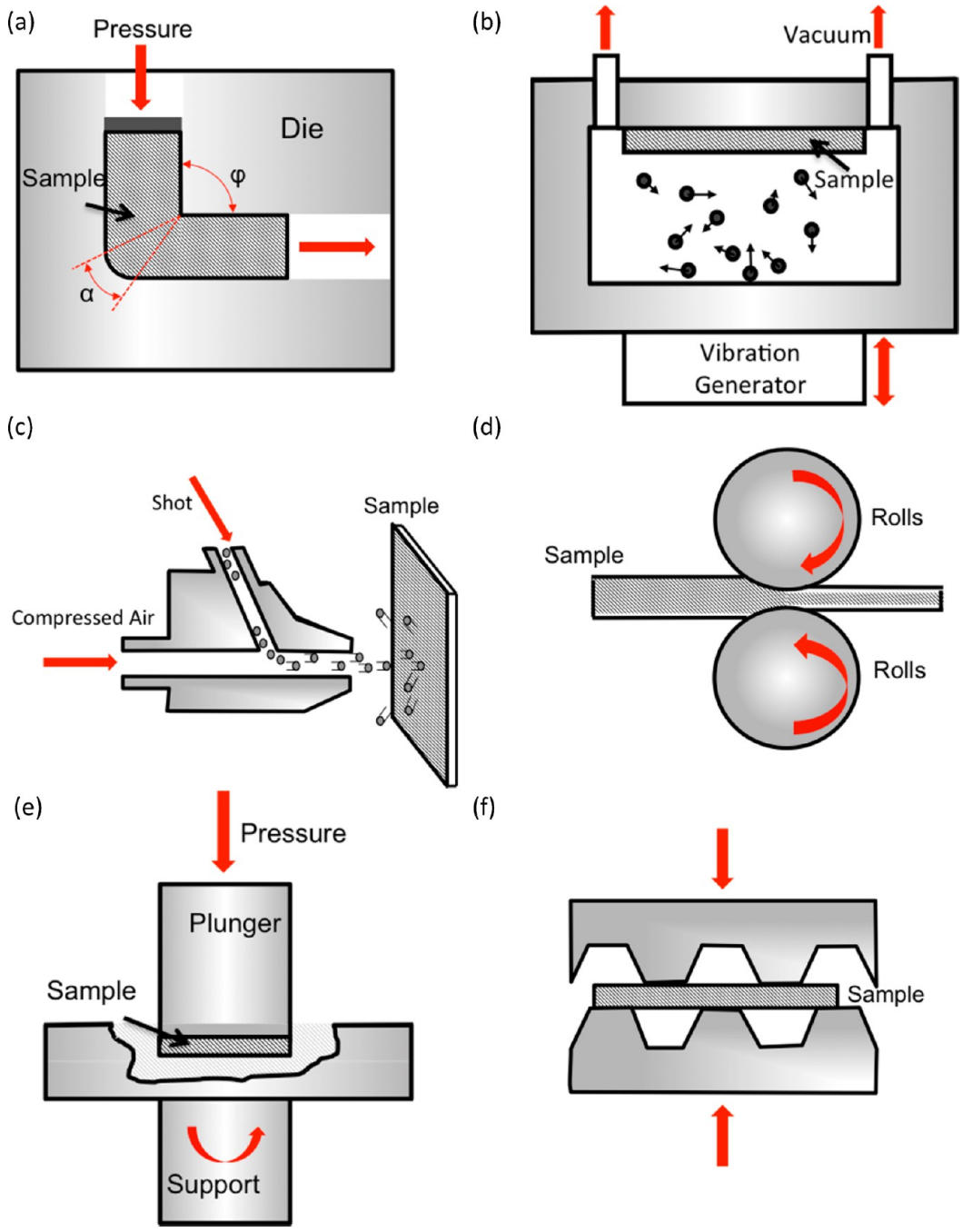

Figure 2. Schematic illustration of SPD techniques: (a) equal channel angular pressing (ECAP), (b) surface mechanical attrition treatment (SMAT), (c) severe shot peening (SSP), (d) severe cold rolling, (e) high pressure torsion (HPT), (f) groove pressing (GP).

ECAP has been effectively applied to large pieces of a wide variety of metals including hard-to-deform Ti and its alloys;[65] the principles of the ECAP technique as well as the grain refinement mechanism have been experimentally and numerically studied on many classes of the materials.[25,40,66−71] The obtained UFG/NG material have demonstrated significant enhancement in mechanical properties including tensile strength,[65,72−76] hardness,[76] thermal stability,[65] ductility,[72−74,77,78] super plasticity,[79,80] corrosion and wear resistance,[81,82] impact and fracture toughness,[83,84] fatigue strength,[84−87] and reduced friction coefficient.[88] In a leading step to commercialize SPD materials in biomedical field, the application of ECAP to obtain UFG structure adapted for medical implants was patented in 2002.[89]

2.2. Surface Mechanical Attrition Treatment. Surface mechanical attrition treatment (SMAT) also known as ultrasonic shot peening (USSP) is the next SPD surface treatment that has been adopted to obtain surface grain refinement on different metallic materials.[90,91] This method is advantageous for cases where there is no need to have bulk NG material, considering that majority of mechanical failures originate from the surface. As illustrated in Figure 2b, the SMAT set-up is practically based on shot peening mechanism.[41] During SMAT, steel balls with smooth surface are resonated in a reflecting chamber via vibration of an ultrasonic transducer

(vibration frequency of 50 Hz to 20 kHz). The diameter of the balls ranges between 1 to 10 mm that is much bigger compared to those typically used for conventional shot peening. The continual multidirectional impacts induce extreme plastic deformation at high strain rates resulting in progressive surface grain refinement down to nanoscale.[92−96]

There are numerous reports of successful application of SMAT to several classes of materials including pure metals, steels, and alloys. Evident enhancement in several mechanical properties and global performance is reported after SMAT treatment including strength,[97] surface hardness,[97−99] wear and friction resistance,[97] corrosion resistance,[100−102] surface wettability,[99] fatigue behavior,[103,104] and convenient nitriding condition.[105−107]

2.2.1. Severe Shot Peening. Severe shot peening (SSP) like SMAT process is based on impacting the surface of the material with high kinetic energy shots. It is an alternative method of shot peening that contrary to SMAT can be performed using the conventional air blast shot peening apparatus and does not require apposite equipment (see Figure 2c). The particular set of peening parameters applied in SSP, enhances the impacts kinetic energy introducing numerous defects, dislocations and grain boundaries on the surface layer of the treated material, and successively transforming its CG structure into NG.[41] The notable advantage of this technique compared to SMAT is that it can be executed with the same equipment that is widely available in the industry for the conventional shot peening treatment.

Experimental and numerical data have confirmed the beneficial role of SSP on mechanical characteristics enhancement for different classes of metallic materials including improvement in fatigue strength, surface hardness, work hardening and residual stress development.[41,44,48,49,51] It is to be mentioned that increasing surface roughness is also an apparent side effect of SSP treatment. Indeed, in concept, SSP is very similar to sand blasting that is commonly used in biomedical applications for surface roughening purposes helping to enhance the bioactivity and early adsorption of extracellular matrix (ECM) proteins on the implant.

2.3. Severe Rolling. Different adoptions of repeated rolling known as severe cold rolling,[63,108,109] accumulative roll bonding (ARB),[47,110,111] and high-ratio differential speed rolling[112,113] have been used to obtain significant grain refinement at different temperatures all through homogeneously induced large shear deformation along thickness of the work piece. Like SSP, the most notable technological advantage of rolling based SPD techniques with respect to the other SPD methods is that they can be implemented using the conventional rolling facility, as presented in Figure 2d.

Rolling based methods have been successfully applied with different combinations of process parameters and condition on many commercially pure metals and their alloys. There are numerous reports of the improved mechanical properties of material treated with such techniques. The particular mechanical characteristics studied are yield and tensile strength,[113−115] electrical conductivity,[112,116] microhardness,[111,117] and stress corrosion cracking.[117,118]

Controlled phase-reversion through severe rolling and annealing, described briefly as following, has also been used as a particular grain refining SPD method. This method has been applied to stainless steels that are of particular interest for biomedical applications and has been used for some studies on cell−substrate interaction.

2.3.1. Controlled Phase-Reversion through Severe Rolling and Posterior Annealing. This technique consists of applying severe rolling deformation of (45−77%) at room temperature to austenite material. The rolling process by itself causes strain-induced transformation of austenite (face-centered cubic γ) to martensite (body-centered cubic α'); after annealing, this martensite transforms back to austenite. The induced recrystallization via annealing process results in significant grain refinement.[119−121] UFG/NG grain refined structure with combined ultra-high yield strength and excellent elongation can be achieved through optimizing the deformation extent as well as the phase-reversion sequence/rate.[122] It is possible to control the obtained grain size range through adopting different combinations of process parameters. This approach is limited to special series of metastable austenitic steels; thus, there are few studies performed on mechanical characterization of the obtained material. However, there are reports of the treated material exhibiting enhanced microhardness,[123] superplasticity,[124] strength and ductility,[122,125] and corrosion resistance.[126]

2.4. High Pressure Torsion. High pressure torsion (HPT) is a SPD procedure in which samples are subjected to extreme plastic deformation through high compressive loads in order of magnitude of several GPa combined with concurrent torsional straining.[127,128] Development of the primary concepts of this method led to the award of the Physics Nobel Prize to Percy Williams Bridgman from Harvard University in 1946;[129] however, it is not long that the actual application of this process for grain refinement became of major importance. The process is schematically depicted in Figure 2e. During HPT a disk shaped sample, is placed in between two anvils where simultaneous extensive compressive load and torsional strain are applied to it. The torsional strain is basically imposed through rotation of the lower anvil.[129]

This method is reported as the most efficient SPD technique for grain refinement with a smaller saturation grain size compared to ECAP[129]—optimizing the extent of compression and number of revolutions of the lower anvil substantiate a uniform and homogeneous distribution of UFG/NG structure.[47,130] However, this technique involves a notable limitation of size and geometry of the samples (disk-shaped samples, normally with a diameter of 10−15 mm and a thickness of 1 mm).

Exceptional properties are obtained through application of HPT to different classes of metallic and intermetallic materials for bulk grain refinement. Among such properties, enhanced strength,[131−135] ductility,[132] superplasticity,[136−138] hardness,[130,139−142] thermal stability,[129] fatigue behavior,[143,144] corrosion resistance,[145] and reduced thermal conductivity[146] can be recalled.

2.5. Groove Pressing. Groove pressing (GP) or constrained groove pressing, developed by Shin et al.,[147] is the most recent SPD technique among the ones described here. It can be considered as one of the simplest methods that provide the possibility of obtaining bulk grain refinement in sheet form material. The schematic illustration of GP is shown in Figure 2f. The sheet form specimen is pressed between a set of dies with asymmetrical grooves that can be firmly constrained by cylinder walls. The next step of pressing using flat dies, applies reverse shear deformation to the previously deformed region. This repetitive shear deformation by alternate pressing between the grooved and flat dies, results in grain refinement to UFG regime.[147,148] In general, GP has lower grain refinement rates than other SPD methods because of its relatively simple

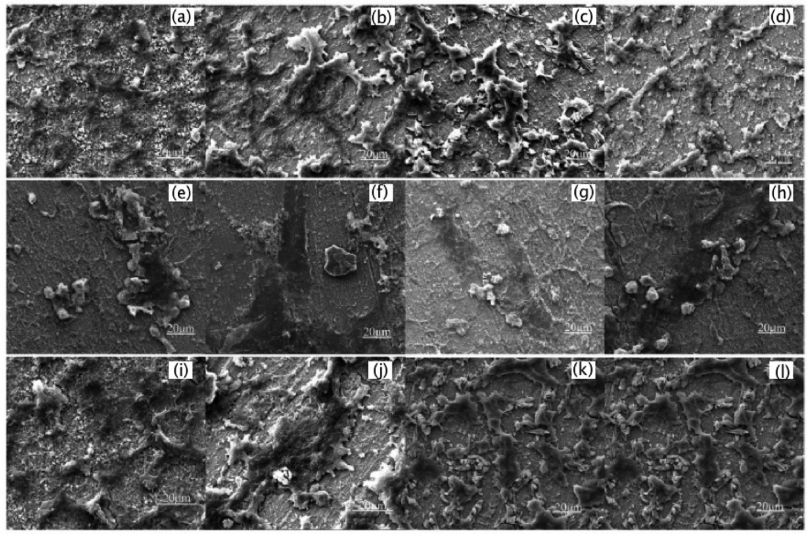

Figure 3. SEM micrographs of cellular morphologies for different cell lines on pure iron samples with gradual grain refinement from left (CG) to right (NG) (a–d) L-929, (e–h) VSMCs, (k–n) ECs.[165] Adapted with permission from ref 165. Copyright 2010, IOP Publishing.

deformation field that induces partial annihilation of the dislocations during groove pressing and successive flattening operations at low accumulated strains.[149,150] The grain refinement rate can be controlled through the optimized choice of die geometry and pressing orientation.

This approach has been successfully applied to few classes of materials such as pure Al, pure Ti and Cu–38Zn alloy. The results of the performed studies have indicated increased tensile and yield strength,[151−153] microhardness,[152,154] improved deep drawability,[155] thermal stability,[156,157] and electrical resistivity.[158]

3. CELL ADHESION AND PROLIFERATION

Cell proliferation and adhesion are known as the basis of in vitro biocompatibility assessment of materials for biomedical implants. Cell adhesion in particular is known to promote the proliferation, differentiation, and expression of specific developmental phenotypes, as well as the osteointegration of the implant. In this section, we will go through the studies that have used NG/UFG material produced by SPD to investigate the cell adhesion and proliferation. The studies are recalled based on the sequence used in section 2 to give a brief explanation on the corresponding SPD technique.

One of the first reports of in vitro cell response on SPD UFG metals was provided by Kim et al.[52] who performed a comparative study on adhesion and proliferation of 3T3 mouse fibroblast cell line on UFG commercial pure Ti processed by ECAP. CG Ti and Ti6Al4V alloy samples were also included for comparison. Different ECAP processes were applied to obtain two series of UFG material (average grain size of 350 and 450 nm). Polishing was performed on all samples' surfaces, to ensure identical surface roughness. Contact angle measurements showed strong grain size dependency, indicating the enhanced wettability in the polished UFG structure.

MTT assay[159] was performed to investigate the fibroblast cell proliferation and viability after 2 and 5 days in culture. MTT is a colorimetric assay for measuring cell activity. Pale yellow MTT substance, tetrazolium dye, is cleaved by the cellular enzymes to its insoluble purple formazan crystals exclusively by viable cells; the concentration of the formazan is regarded as an index of the number of metabolically active cells.[159,160] Significant increment in the cell proliferation was reported on UFG samples compared to CG Ti, particularly after 5 days in culture (~61% and ~40% higher than CG Ti and Ti 6Al4 V alloy samples, respectively). Smaller grain size substrates showed higher adhesion (after 16 h) and proliferation values (up to 5 days). Moreover, the cytotoxicity tests did not reveal any significant difference between UFG and CG materials.[53]

It is interesting to note that cell adhesion profile corresponded to the respective wettability characteristics of different substrates. Taking into account that all samples were mechanically polished and had identical surface topographies, the cell adhesion enhancement was considered as a result of the higher surface energy, wettability, and feasibly the presence of numerous nanoscale conical groove-like structures (at point junctions of grain boundaries) on the surface of the UFG Ti sample in comparison with the CG Ti and Ti6Al4V samples. This tendency was confirmed in another work by the same group in which the same fibroblast cell line adhesion on ECAP processed pure Ti (grain size of 240 nm) was assessed.[161] Cell adhesion was quantitatively analyzed by immunolabeling the extracellular protein fibronectin and the highest signal was detected for UFG Ti substrates.

Valiev et al. studied the adhesion of L929 mouse fibroblast cells on NG grade 4 commercially pure Ti produced by ECAP (grain size of 150 nm). The samples' surface was preliminarily etched in hydrofluoric acid to obtain rough surfaces that are known to be favorable to cell adhesion. The results of this study indicated that fibroblast colonization of the samples' surface dramatically increased by grain refinement. The cell density on CG Ti (25 μm) was 53% after 72 h in culture compared to 87.2% for UFG Ti samples.[162,163] However, due to different surface topographies, the observed results cannot be directly attributed to grain size effect.

Proliferation of preosteoblastic MC3T3-E1 cells extracted from mice embryos was studied on UFG pure Ti (grain size of 200 nm) processed by ECAP and compared to as-received CG material (grain size of 4.5 μm).[164] Also, in this case, MTT assays after 7 and 12 days in culture demonstrated notable enhancement of cell proliferation and viability on UFG samples compared to the CG material.

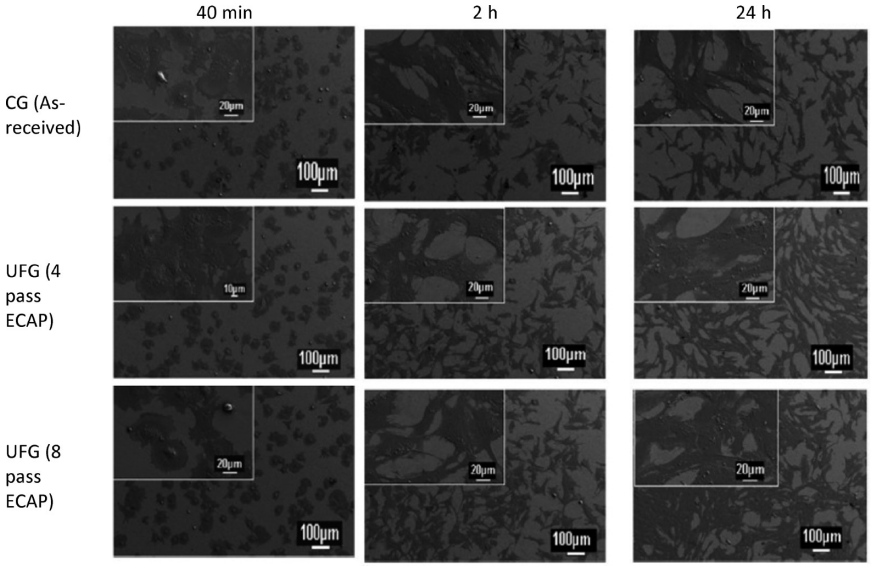

Figure 4. SEM micrographs of hMSCs morphologies on CG and UFG ASTM Grade 2 pure Ti.[166] Adapted with permission from ref 166. Copyright 2011, Elsevier.

The in vitro interaction of different cell lines on NG pure iron samples was studied for the first time through application of ECAP. Biodegradable medical devices such as cardiovascular stents made of pure iron that is a well-known body-friendly and indispensible micronutrient are of significant interest. In order to overcome pure iron's shortcomings as endothelialization fulfillment, structural failure or restenosis caused by the struts thickness that narrows the blood vessel, the application of a SPD treatment and grain refinement of pure iron was studied as a potential solution.[165] Different ECAP process parameters were implemented to obtain gradual refinement in the microstructures (from 40−50 mm to 80−200 nm) and to consider the effect of this refinement on cellular response and hemocompatibility of the samples. The acceptable hemolysis rate of less than 5% was observed for both CG and NG pure iron samples. The nanostructure turned out to be able to intensely suppress the burst of red cells and the attachment of the platelets to the NG pure iron samples. Cell viability and spreading studies were performed through indirect assays as well as direct cell seeding on the samples. UFG/NG pure iron samples presented preferential cellular response to different cell types including murine fibroblast cells (L-929), vascular smooth muscle cells (VSMCs), human umbilical vein endothelia cells (ECs), and human umbilical vein endothelia cells (ECV304). As it can be observed in Figure 3, good spreading and viability were observed for L-929 and ECs with a grain size dependent trend: while VSMCs showed less activity and not noticeable proliferation, less than 60% cell spreading for VSMCs vs over 80% for the other cell types after 4 days in culture.[165]

Later, Estrin et al.[166] studied the attachment and spreading of human bone marrow-derived hMSCs to the surface of CG (4.5 mm) and ECAP processed UFG (170-200 nm) ASTM grade 2 pure Ti. Two different sets of process parameters (4 passes and 8 passes) were applied to obtain UFG Ti with different grain size. The adhesion and spreading of hMSCs in the initial phases (for up to 24 h in culture) was positively affected by grain refinement. The microscopical observations revealed differences in adhesion of hMSCs to different surfaces even within the first 40 mins; stimulated spreading was observed particularly on UFG series of samples showing up to 2.5 times greater biovolume for hMSCs on UFG Ti compared to the CG material. Figure 4 clearly indicates that hMSCs attached and spread more readily on UFG samples compared to the CG one.

Since the atomic force microscope revealed different surface topography on the nanoscale for the as-received and ECAP processed material after being mechanochemically polished, it was postulated that the enhanced hMSCs adhesion and spreading on UFG samples was majorly attributed to the surface topography alterations at nanoscale. It is stated that the surface of UFG material was characterized with more densely spaced and the more frequent peaks on the nanoscale that increased by decreasing the grain size; these aspects were regarded to have the potential to manipulate cell response to the substrate.[166,167]

In another study, cell adhesion and proliferation of osteoblast-like cell line MG63 were studied on UFG $Ni_{50.8}Ti_{49.2}$ alloy fabricated by ECAP process.[14] Before cell seeding, the obtained UFG samples had gone through different combinations of surface treatments such as sandblasting, acid etching, and alkali treatment to obtain irregularly roughened surface, microporous surface, and hierarchical porous surface, respectively. Surface modification improved general cytocompatibility and apatite-forming ability, although the cell activities were differently affected by each individual surface modifying technique. Sandblasting enhanced cell attachment after 4 h, while sand blasting followed by HF/HNO_3 solution etching promoted cell proliferation, with higher number of cells after 9 and 14 days. The dissimilar cellular responses to UFG samples treated by different approaches were mainly influenced by the surface topography and hydrophilicity alterations of the oxide layer formed on the surface—thus again impeding the possibility of determining grain size effect individually.

The effect of combined sandblasting, acid etching, and alkali treatment implemented to generate a hierarchical porous surface on ECAP processed UFG commercial pure Ti was also studied by Zheng et al.[169] In this case, the hierarchical porous surface enhanced osteoblast-like MG63 cells adhesion and proliferation. The results demonstrated increased cell attachment to surface modified UFG Ti samples compared to

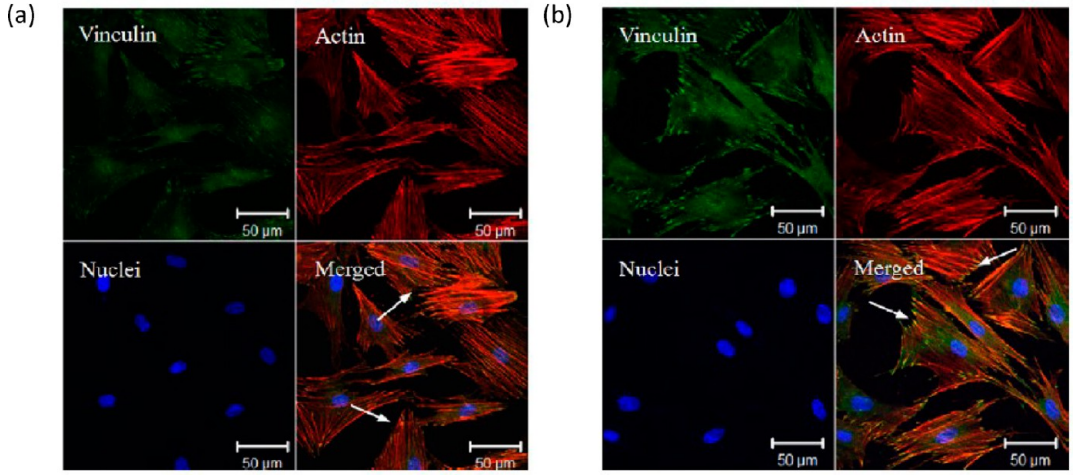

Figure 5. Fluorescence microscopy images of MSCs on (a) CG Ti (b) NG Ti. Cells stained with actin filaments (red), cell nuclei (blue), and vinculin (green).[174] (For interpretation of the references to colors, the reader is referred to the web version of the article.) Adapted with permission from ref 174. Copyright 2012, Elsevier.

smooth UFG and smooth CG samples at early stage of cell culture (4h); while after 24 h no statistical difference was observed between the three series. In terms of proliferation both smooth and surface modified UFG series showed notably higher proliferation in comparison with the CG Ti surface at day 9, while relatively comparable data was obtained at day 3 and 7.

In an attempt to overcome the problems involved with application of CG copper intrauterine devices (IUD) that is burst release and the low transfer efficiency of the cupric ions, Xu et al.[170] studied the possibility of substituting them with UFG copper produced by ECAP. In vitro experiments were designed to assess the cytotoxicity of the UFG (260 ± 10 nm) and CG (40 ± 5 μm) copper samples to murine fibroblast cells (L-929). MTT assay results after 3 days in culture, represented improved cell viability on UFG samples compared to the CG ones.

SMAT treatment was also applied in some similar studies. Ti6Al4V samples were SMAT treated[171,172] and subsequently electrochemically polished using an acidic corrosion solution to produce a porous structure on their NG surface. Neonatal rat calvarial osteoblasts adhesion to NG and CG rough surfaces was studied. Notably higher cell attachment was observed for the NG surfaces after 6 and 24 h in culture compared to the CG ones. Only after 2 h in culture, noticeably spread cells with multidirectional strong attachment were observed on the NG substrates compared to the spheroidical morphology that was observed on the CG smooth substrate. The growth curves provided up to 14 days in culture demonstrated that the osteoblasts had not only higher but also longer growth phase for cell proliferation on NG surface in comparison with those cultured on the CG surface.[172]

Enhanced cell attachment and viability were observed also for Saos-2 cells (human osteosarcoma cell line) seeded on SMAT treated pure Ti compared to the CG Ti substrates.[173] After 8 h in culture, actin filaments exhibit extensive spreading on the SMAT treated substrate, and the cells display flattened shape, in contrast to the almost spherical morphology of the cells on the CG substrate. MTT results after 1 and 3 days also showed statistically higher cell viability on SMAT treated series compared to the CG ones.[173]

Effect of surface nanocrystallization obtained through SMAT treatment was examined also on MSCs attachment, spreading, and viability.[174] MSCs isolated from bone marrow of rat femur and tibia were seeded on NG and CG Ti substrates. SEM and confocal microscope observations after 2 days in culture showed cells spread better with numerous integral pseudopodia outspreading on the NG surface in comparison with the ones on the CG surface.

With special attention to the fact that the ECM proteins are known to mediate cell−substrate interactions and affect the cell cycle including adhesion, proliferation, viability and differentiation, later on, many researchers focused on studying the development and organization of different proteins involved in cell adherence including fibronectin, actin, and vinculin. Triple staining of actin (cytoskeleton), vinculin (focal adhesion protein), and nuclei, shown in Figure 5, demonstrate that the MSCs cultured on the NG Ti display outspread morphologies and well-developed actin stress fibers compared to the cells adhered to the CG surface. Higher vinculin expression was also observed for the cells on NG substrate.

The day 1 results of MTT assay were almost the same for all Ti samples, while higher cell viability was detected on the NG Ti surfaces in comparison with the as-received CG Ti surfaces, at day 3, day 5, and day 7.[174]

The other SPD treatment applied to generate surface nanocrystallization of biomaterials that is investigated in terms of cell substrate interaction is severe rolling. This treatment was applied to Zirconiom (13 μm) to obtain UFG Zr (240 nm).[175] Water contact angles showed comparative hydrophilicity for the CG and UFG samples (73 ± 2 vs 68 ± 3, respectively). Cell adhesion and proliferation were studied using human osteosarcoma Saos-2 cells. In these experiments, the grain size refinement turned out to affect neither the number of the attached cells nor their morphology. Fluorescence microscopy images revealed comparable cell spreading on both surfaces (see Figure 6). Cell viability was examined using Alamar Blue assay up to 7 says in culture. The AlamarBlue assay is used to measure proliferation and viability as it quantifies the reducing ability of the intracellular environment. Metabolically active cells reduce the weakly fluorescent blue cell permeable ingredient of AlamarBlue, resazurin, to the pink highly fluorescent resorufin. The extent of

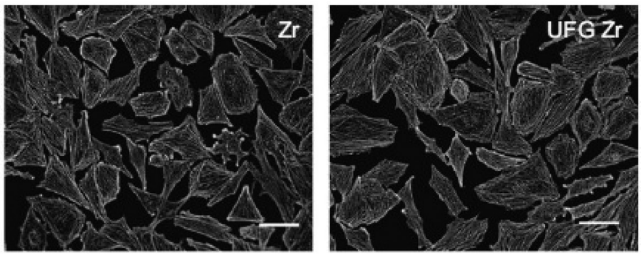

Figure 6. Actin stained Saos-2 cells on CG and UFG zirconium surfaces after 24 h.[175] Adapted with permission from ref 175. Copyright 2007, Elsevier.

Alamar Blue reduction can be correlated with the metabolic activity of the cells.[176] The AlamarBlue results indicated similar level of proliferation for the cells on both the UFG Zr and CG Zr at all time points up to 7 days.[175]

Severe rolling was also applied to 304 stainless steel to generate grain refinement up to 50 nm. Different cells of murine and human cell lines from oral and endothelial environment were co-cultured with extracts for up to 4 days to estimate the in vitro cytotoxicity by indirect contact.[177] The proliferation trend of all cell lines exhibited comparable viability on NG and CG substrates; no notable difference was observed for the cell viability on different substrates up to 4 days in culture. However, the overall proliferation represented the excellent non-cytotoxicity of the NG substrates.

A more recently developed approach based on SPD that is studied in terms of grain refinement effect on cell behavior is the combined severe rolling and annealing process that involves controlled phase reversion. This method has been applied in studies using preosteoblasts suggesting that preosteoblast cells response is considerably affected by substrate's grain structure. Mouse preosteoblast MC3T3-E1 cells were cultured on austenitic steel substrate (52 μm) and different severely rolled substrates including NG (<100 nm), UFG (100−500 nm), and some sub-micrometer (500−1000 nm) grains.[178−180]

Cell adhesion and viability on CG and NG/UFG substrates was evaluated by MTT assay for up to 7 days in culture. Enhanced cell attachment (evident within the first hours in culture) and cell metabolism were observed on UFG/NG substrates. The cells were reported to present a more compact morphology on CG substrate whereas the cells on NG/UFG substrates exhibited a flat and more extended morphology, in some cases showing a star-shaped arrangement with several cytoplasmic extensions. Immunofluorescence microscopy observations indicated higher expression and distribution of vinculin and better organization of developed actin filaments on UFG samples. Fibronectin expression was similarly promoted on NG/UFG steel in comparison with CG steel substrates. At day 2, well-defined stress fibers were observed on NG/UFG surfaces. The results implied that cell adhesion, morphology, and growth were all affected by grain size.[178]

Preosteoblast cells were also cultured on UFG stainless steel samples obtained through controlled phase reversion and subsequent electrochemical etching. The results, probably more directly affected by the induced surface topography, showed notably improved adhesion, proliferation, and viability of preosteoblast cells on rough surfaces compared to the smooth NG/UFG surface.[8]

The same grain refinement process was performed on a low Ni bearing 15Cr9Mn1.7Cu steel (22 μm),[62] to obtain grain refinement down to a combination of NG (d<200 nm) and submicrometer grains (200−1000 nm). Cell adhesion, proliferation, viability, and quantitative analysis of select proteins expression (fibronectin, actin, and vinculin) indicated that the latter parameters were favorably enhanced on UFG samples. These observations were confirmed by evaluation of cytoskeletal development, cytomorphometry (cell area, perimeter, and Feret's diameter analysis), and expression of the focal adhesion proteins by immunofluorescence microscopy. Comparison of cell morphology on different substrates revealed promoted cell adhesion and well spreading on the UFG substrate with numerous cytoplasmic extensions developed soon after early hours of incubation. On the other hand, more localized and less spread cells were observed on CG substrates, after 1 h in culture. This significant difference was notable also after 24 h in culture. It was concluded that reduction of Ni content in stainless steels compared to the conventional material used for bioimplants, has the potential to promote cell functions.

Also for fibroblast cells, initial adhesion, proliferation, viability, and morphology on stainless steel treated by combined severe rolling and annealing process are reported to be notably affected by grain size.[181,182] Significantly higher number of cells was observed on NG/UFG substrates compared to the CG samples after 1, 2, and 4 h in culture. Apparent difference is also reported on the morphology and spreading of the fibroblasts on different surfaces showing accelerated spread and growth on the NG/UFG substrate (see Figure 7). After 4 and 24 h in culture, cells with greater extent

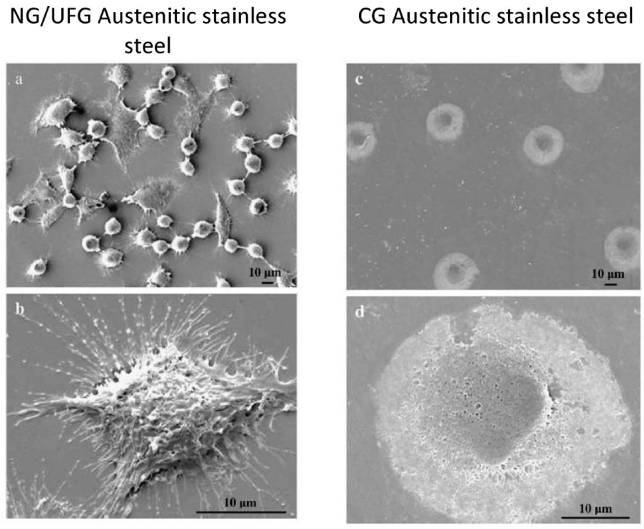

Figure 7. SEM micrograph of L-929 morphology on 316L stainless steel after 1 h in culture: (a and b) NG, (c and d) CG.[182] Adapted with permission from ref 182. Copyright 2010, Elsevier.

of spreading and denser extracellular matrices and more cell-to-cell contacts were detected on NG/UFG substrates.[182] Moreover, higher expression of fibronectin, actin, and vinculin was observed on UFG surface at early stages of culture.

Protein absorption studies were performed on 301LN stainless steel processed by severe rolling and reversion annealing to obtain grain refinement from 22 μm up to 500 nm.[183] Water contact angle was decreased from 75.14 ± 5.34° for CG to 66.01± 2.19° for NG/UFG substrates. The interaction of bovine serum albumin (BSA) with the surface was studied via scanning electron microscopy. Higher

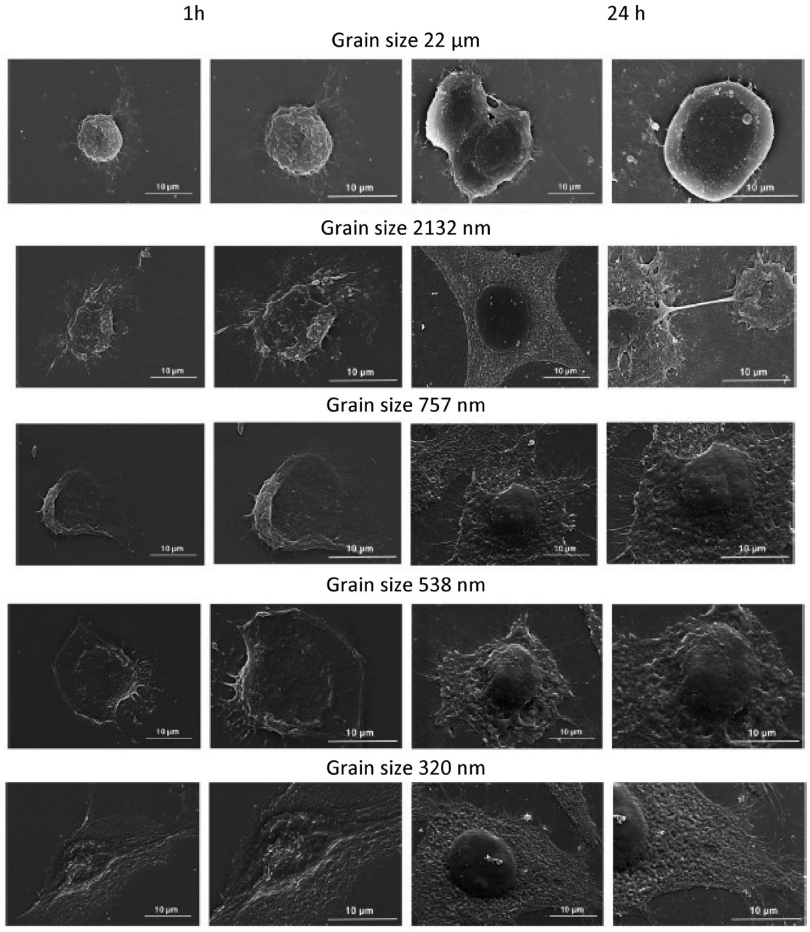

Figure 8. SEM micrograph of MC3T3 morphology after 1 and 24 h in culture on 316L with different grain sizes.[184] Adapted with permission from ref 184. Copyright 2013, Elsevier.

concentration of BSA was measured on the UFG substrate following the hydrophilicity trend of the two surfaces. Cell functions were then studied on the protein absorbed CG and UFG surfaces using mouse preosteoblast MC3T3-E1 cell line. Remarkably higher cell attachment was observed on protein-adsorbed surfaces compared to the respective bare counterparts. Higher cell metabolism was also measured on UFG materials by MTT assay. Irrespective of prior protein adsorption on the surface, NG/UFG surfaces promoted cells viability in comparison with both bare and protein adsorbed CG substrates. The fibronectin expression, actin stress fibers and vinculin focal contacts followed the same trend, that is, NG = UFGBSA > NG > CGBSA > CG after 2 days in culture. Overall the prior protein adsorption turned out to affect the cell response to the substrate; however, since CG substrate with protein showed lower cell adhesion in comparison with the bare NG surface, it is concluded that protein adsorption, although beneficial, is not sufficient to positively modulate the cells response to the substrate, thus confirming again the dominant effect of substrate structure on cell attachment.[183]

Misra et al. in their recent study applied severe rolling and subsequent reversion annealing with different process parameters (altering the extent of rolling and annealing temperature−time sequence) on 316L samples to obtain gradual grain refinement starting from NG scale to the CG scale; the obtained samples were used to demonstrate the impact of grain structure on MC3T3 pre-osteoblast cells activity.[184] Surface of samples were mechanically polished to obtain similar surface roughness—water contact angle measurements indicated a decrease in surface wettability from 78° to 52° with grain refinement from an average of 22 μm (CG) to 320 nm (NG); MC3T3 cells on UFG and NG samples showed more elongated/star-like morphologies with several cytoplasmic extensions after 24 h in culture. Cell spreading pattern and cell morphology were reported to be significantly affected by grain structure after 24 h in culture. As shown in Figure 8, the cells represented compact and almost spherical morphologies on CG samples and as the grain size decreased the extent of spreading increased. Viability tests (MTT assay) indicated strong effect of grain structure, showing an increasing viability trend by decreasing grain size up to 7 days in culture.

Individual proteins (fibronectin, actin, and vinculin) expressions confirmed the favorable effect of grain refinement, following the same trend of cell attachment data. At early stages, higher vinculin expression and well developed more extended actin stress fibers were reported on NG samples compared to CG ones (see Figure 9). These observations also follow the same trend as cell adhesion and viability, that is, grain refinement turns out to be favorable also to these parameters.

Grain refinement (from 9 mm to 10−50 nm) was obtained on Ti substrates through HPT process.[185] Interaction of such surfaces with mouse pre-osteoblast MC3T3 cells and rat fibroblast Rat1 cell lines were studied in terms of cell attachment, growth rate, and cell activity. Improved pre-osteoblast cell adhesion and growth rate on HPT samples

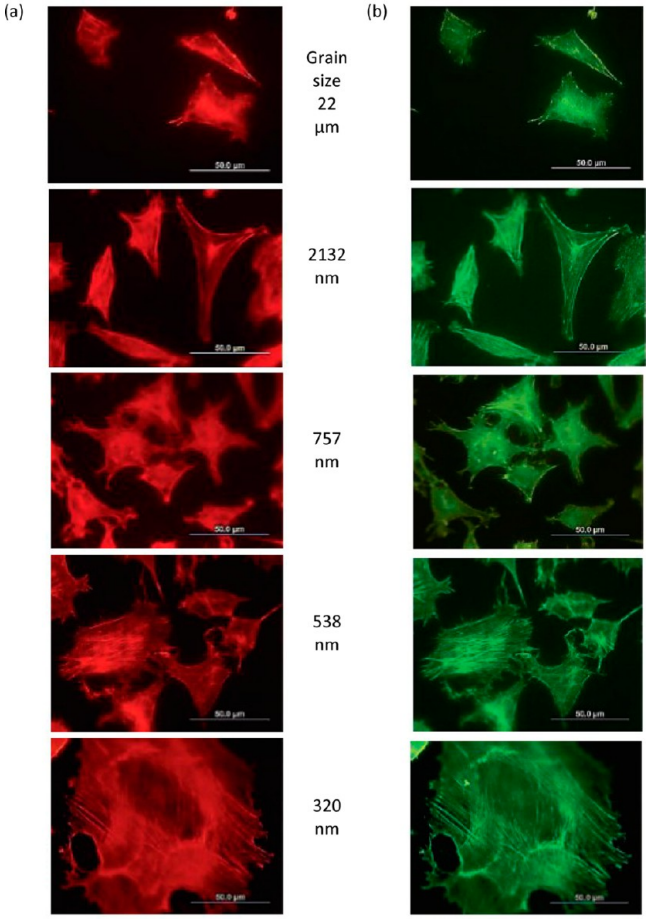

Figure 9. Fluorescence micrographs of vinculin focal contacts (a, column) and actin stress fibers (b, column) of MC3T3 pre-osteoblast cells on austenitic stainless steel of different grain sizes after 48 h in culture.[184] (For interpretation of the references to colors, the reader is referred to the web version of the article.) Adapted with permission from ref 184. Copyright 2013, Elsevier.

indicated that the cell interaction with the NG substrates was highly regulated by the grain structure. Extracellular proteins expression was also analyzed quantitatively and qualitatively; immunofluorescence microscopy revealed strong vinculin signals connected to the actin stress fibers on the edges of the cells and along the cellular extensions on NG surfaces, while less intense vinculin expression was detected on CG samples. Higher density of pre-osteoblast cells was measured on the surface of NG samples. In contrast, the fibroblasts showed a statistically significant less adhesion to NG substrates at all time-points. Taking into account that presence of fibrous tissue at the interface of the implant and bone, can result in loosening the preferential attachment of pre-osteoblasts, this observation is considered as an additional advantage of the HPT processed NG Ti.

It is interesting to note that in this case, XPS and XRD studies revealed a clear shift in the composition or structure of oxide layers of 2−6 nm thick developed on the surface of different Ti samples, which was supposed to be affected by grain size. This issue is assumed to result in different wettability. Since the samples are reported to have similar crystal orientation and surface topographies, different cell responses to the substrates were attributed to the different surface wettability that are associated with the dissimilar surface oxide layers.[186]

Another study was performed on the cytotoxicity and cell interaction of murine fibroblast (L929 cell) and osteoblast (MG63) cell lines with bulk NG $Ni_{50.2}Ti_{49.8}$ alloy samples prepared from commercial CG $Ni_{50.2}Ti_{49.8}$ alloy discs through HPT.[187] Despite the outstanding characteristics as shape memory effect and super plasticity of NiTi alloys,[188] their application in biomedical fields is very limited due to the potential of releasing toxic non-zero covalent nickel ions in the body fluid environment as a cause of bio-corrosion or erosion.[189] Grain refinement has been applied to this class of materials with the aim to eliminate/minimize this shortcoming. In this case, the tests indicated no cytotoxicity for murine fibroblast and osteoblast cell lines indirectly co-cultured with the samples' extracts. Cell viability and proliferation measured via MTT assay up to 4 days in culture did not show any notable difference between the CG and NG substrates response to L-929, while in case of MG63 slightly higher viability was measured on NG substrate.

As mentioned before, magnesium alloys application in biomedical field is highly limited by the weakening effect of high corrosion rate and consequent hydrogen bubbling on cell activities.[190] GP has been applied to optimize the degradation rate of magnesium alloys exposed to body fluids especially in the early stages of exposure. Grain refinement down to 7 μm in AZ31 magnesium alloy was achieved from an initial grain size of 55 μm.[191] The samples were immersed into super saturated simulated body fluid (SBF) solution to evaluate the degradation rate. X-ray diffraction results indicated early deposition of precipitates composed of HA, magnesium phosphate and magnesium hydroxide on GP treated UFG substrates compared to the CG ones with no evident peaks corresponding to HA or magnesium phosphate for CG samples even after 48 h of immersion. The results imply the enhanced bioactivity of GP processed substrates. More and wider surface cracks were detected on the as-received CG substrates by time, indicating that the GP treated samples had a lower degradation rate. Substrate interaction with rat skeletal muscle (L6) cells was investigated. MTT assay results indicated nontoxicity of both GP treated and as-received CG samples, with no statistically relevant difference between the samples. However, cell morphology studies indicated enhanced cell adhesion and spreading on GP treated samples compared to the CG series. It is concluded that the improved cell adhesion to the GP treated samples is due to their higher surface hydrophilicity and lower degradation rate that favor the cell attachment. It is to be noted that in this study the CG and as-received samples have different surface roughness (increased from 0.16 ± 0.02 μm to 2.53± 0.3 μm), different grain size (55 um vs 5 um), and different surface wettability (77.13° ± 1.13 vs 61.58° ± 1.22).[191]

4. MINERALIZATION AND DIFFERENTIATION

Improvement in osteoblast functions such as differentiation and mineralization is a prerequisite for achieving eventual osteointegration of implants in vivo. The aforementioned studies were mostly focused on short-term cytotoxicity and fewer studies have established the late osteoblastic cell functions on UFG/NG substrates obtained through SPD. Considering the significance of binding characteristics of the implant material to the living bone and its osteoconductive properties, in this section, we will go through the studies

conducted on the role of SPD material in promoting bone matrix maturation and mineralization.

Park et al.[192] performed in vitro experiments demonstrating the late osteoblastic cell behaviors on UFG pure Ti (ASTM Grade 2) substrates produced by ECAP using MC3T3-E1 cells (mouse calvaria-derived osteoblast-like cell line). Conventional CG pure Ti and Ti6Al4V substrates were also used as control. All Ti surfaces including UFG (200−300 nm grain size), CG pure Ti and Ti6Al4V (24 and 13 μm grain size respectively) were grit-blasted using HA particles to induce micro roughness on the surfaces before cell seeding. The surface microroughness measurements showed alike surface topography in terms of standard surface roughness parameters for the samples after grit blasting. It is well-recognized that microrough surfaces boost the potential of achieving rapid and strong osteointegration.[193,194] During early culture time, improved cytocompatibility and promoted cell attachment and spreading, were observed for UFG surfaces. Distinct alkaline phosphatase (ALP) activity, as an early marker of osteoblast differentiation, was quantified on UFG substrates.[195] As a mineralization-associated protein for osteogenesis of osteoblasts, ALP is taken as a prominent indicator of cells' early osteogenic differentiation tendency. Considering the relevance of rapid regeneration of new bone in the interface with the implant surface, calcium deposition is a crucial parameter for evaluation of osteointegrity of the implant material. Osteoblastic gene expression was quantitatively analyzed at day 7 in culture. Both set of the early markers (ALP, osteopontin) and terminal marker (osteocalcin) were expressed to higher extent on UFG surfaces compared to CG surfaces. Intense Alizarin Red S staining showed more mineralization nodules on the UFG and CG Ti surface compared to the control Ti6Al4V surfaces; no statistical difference was reported for the CG and UFG substrates.[192]

Zhao et al. applied stable isotope labeling with amino acids in cell culture (SILAC), as a metabolic labeling technique in proteomics, to study the biological effect of grain size on human osteoblasts at the whole proteome level.[196] Human osteoblast-like MG-63 cells were seeded on UFG grade 4 pure Ti processed by ECAP. The cytocompatibility assay did not reveal any notable difference in the cell attachment and proliferation on CG and UFG samples up to 7 days in culture. SILAC procedure was implemented to assess and quantify the global protein expression of osteoblast proteome, after 14 days in culture. The results indicated of no significant overall change in the proteome on different substrates. Few over-expressed proteins were detected in differentiated osteoblasts on UFG samples; however, proteins with more than a two-fold alteration in osteoblast proteome were less than 4%. Similar ALP activities were also reported for cells on UFG and CG substrates after 14 and 21 days in culture. Overall the results put forward negligible role of grain refinement on osteoblast cells at the global protein level in this study.[196]

ECAP was applied on commercially pure Ti grade 4 (10−30 μm) to obtain grain refinement up to 250 nm and study its effect on the cell attachment, cytotoxicity and differentiation.[197] Static immersion in the SBF was performed to evaluate the adhesion of HA-like precipitates to the UFG and CG substrates. Energy dispersive X-ray spectrometry detected bone-like apatite depositions on the surface of UFG samples, while for the CG samples only few particle sediments were observed after 14 days in culture. Cell−substrate interaction was studied using murine fibroblast cell lines (L-929), osteoblast cell lines (MG63), vascular smooth muscle cells (VSMC), and endothelial cells (ECV304) for indirect viability evaluation, while MG63 was co-cultured with the samples to evaluate the direct interactions of the cells with the substrate. Preferential attachment and viability were observed: the results indicated inhibition for fibroblast and proliferation for osteoblast cell lines. Nevertheless, the cell proliferation was comparable for all four types of cell lines on the UFG and CG samples.[197] The ALP activity was promoted on UFG samples and eventually after 21 days in culture, mineralization on the UFG samples showed a marginally higher alizarin red staining compared to that on CG substrates.

Zhao et al.[198] performed in vitro mineralization study on Ti6Al4V substrates treated by SMAT. The SMAT treated samples showed notably lower contact angle, that is, higher hydrophilicity with respect to the CG as-received material. Higher extents of calcium and phosphorous minerals precipitation were reported on the NG substrates after immersion into SBF up to 21 days. Considering both effects of grain size and surface roughness, the results indicated higher apatite forming ability of the NG substrates. Neonatal rat calvaria osteoblast cells were seeded on both substrates to investigate the cellular mineralization. Although the number and morphology of mineralized bone-like nodules were similar on both surfaces after 14 days, a significantly larger area was covered by them on the NG surface compared to that on the CG samples.[198]

Cell differentiation and calcium deposition was also investigated on SMAT and acid etched Ti6Al4V substrates.[172] The ALP activity of the cells on the obtained NG Ti6Al4V substrate was found to be higher than the CG material. It is reported that the average number of the calcified nodules was similar on both substrates after 14 days in culture; however, a significantly larger size of calcified nodule was observed on NG material.[172]

Cell differentiation was examined through ALP activity and bone mineralization of MSCs on surface nanocrystallized pure Ti treated by SMAT treatment.[174] Significantly higher ALP activitiy was reported for the cells on NG Ti in comparison with the CG Ti substrates at day 7, 14, and 21 of culture. Alizarin red staining after 21 days in culture displayed expressively higher mineralization on the NG Ti compared to CG substrates.[174]

The differentiation ability of hMSCs from bone marrow cultured on Zirconiom substrates treated by severe rolling was assessed through analyzing the ALP activity and mineralized nodule formation. After 18 days in culture no notable difference was detected between the ALP activity and mineralization extent of cells on the CG and UFG Zr samples; also, similar cell adhesion, morphology, and viability were reported.[175]

Apatite forming ability was studied also on ECAP treated Ni50.8Ti49.2 alloy[14] and pure Ti,[169] which subsequently went through a series of surface treatments as sandblasting, acid etching, and alkali treatment to generate irregularly roughened surface, microporous surface, and hierarchical porous surface, respectively. The samples were immersed in SBF (pH of 7.4). It was reported that the increased surface area obtained through surface modifying techniques stimulated the incorporation of calcium and phosphate ions and consequently enhanced the apatite materialization and deposition rate. However, it is not stated whether the observations are due to the presence of NG or the particular surface topography induced through additional surface treatments.

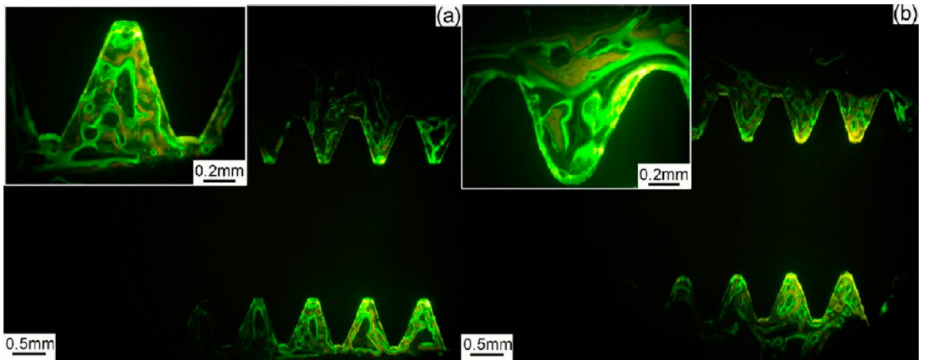

Figure 10. Histotomy of bone around the Ti implant after 4 weeks: (a) CG Ti; (b) UFG Ti. Illustrated by fluoresecence-dyeing reagents, where yellow represents 1 week formed new bone dyed by tetracycline, pink represents 2 weeks formed new bone dyed by clacein, and green shows 4 weeks formed new bone dyed by calcein-blue.[197] (For interpretation of the references to colors, the reader is referred to the web version of the article.) Adapted with permission from ref 197. Copyright 2013, John Wiley & Sons.

5. IN VIVO STUDIES

In vitro studies provide substantial data on the preliminary screening of biomaterials, however, the actual clinical relevance of any material to be used for biomedical implants must be evaluated in controlled clinical in vivo studies, before any solid conclusions are drawn on their biocompatibility. Nevertheless, there are very limited in vivo studies on material with refined grains obtained through SPD approaches and few researchers have taken the steps forward to perform in vivo studies after performing in vitro examinations on their materials.

One of the first in vivo studies on UFG material obtained through SPD was performed by Bindu et al.[161] They applied the ECAP process on commercially available ASTM grade 2 pure Ti to perform in vivo studies on the properties associated with grain size of the material and their effect on cell−substrate interactions. Their work focused on the biocompatibility of UFG and CG Ti, by quantitatively assessing inflammatory cells, especially macrophages surrounding the implant site, using immune histochemistry and image analysis. The number of macrophages at the peri-implant site was considered as an indication of the response elicited by the material.

UFG metals were implanted subcutaneously in Wistar rats. The implants with the surrounding tissue were retrieved and histological analysis was performed after 30 days post implantation. An immune-histochemical assay was carried out to detect the number of macrophages in the peri-implant tissue. Smaller number of inflammatory cells, especially macrophages in the implant interface with the surrounding tissue for UFG Ti compared to CG Ti, indicated that UFG Ti was less immunogenic. It is mentioned that interactions at the materials-macrophage interface triggers macrophage activation leading to the production of pro-inflammatory signaling molecules responsible for the extended immune response. Thus, the higher number of macrophages observed in CG Ti can emphasize a prolonged inflammatory response compared to UFG Ti.

In another study, Valiev et al. reported the production of ECAP produced NG Grade 4 pure Ti intraosseal dental implants with reduced diameter compared to CG counterparts. It was also stated that clinical application on over 250 patients, showed no adverse effects and excellent primary stability.[162,163]

Another in vivo study was performed by Nie et al.[197] on ECAP processed grade 4 pure Ti. Thread-structured samples were implanted in matching holes drilled into the tibia of rear leg of Beagles dogs for up to 12 weeks; CG Ti implants were also used as control. Threaded cylindrical samples were removed 1, 2, 4, 8, and 12 weeks after implementation. Section histomorphometry analysis, micro-CT scanning and final 3D-reconstruction images were performed to evaluate the response of cells to the implant at the interface. Neo-formed bone around the NG Ti implants turned out to undergo the thorough transformation cycle from osteons or immature woven bone to mature lamellar bone (skeletonic trabecular) after 12 weeks. Higher amount of bone mineral density was observed around the NG implant compared to the CG Ti implant in the first few weeks. After 12 weeks implantation, the NG implant group presented notable osteointegration displaying direct implant-bone contact with no fibrous tissue encapsulated in the interface of the implant and the bone.

Figure 10 represents the fluorochrome-dyeing images that display the configuration of newly formed bone up to 4 weeks after implantation for both groups of the implants. The onset of 1-week bone (yellowish color) formations can be observed in Figure 10, while the 4-week bone (green color) grows maturely forming the major skeleton. It is postulated that the UFG implant promotes rapid bone formation and relatively facilitates post-surgery recovery.

SMAT treated Ti6Al4V was implanted in New Zealand white rabbits posterior limb for up to 12 weeks.[198] Defects were drilled in the femora trochanter from the medial direction at double femur posterior limb. The NG and CG Ti6Al4V implants were placed in the defects made beforehand. After 12 weeks the bone samples of implants were harvested. The histology observations showed the presence of regularly arranged newly formed bone matrixes surrounding the NG implant, whereas undesired fibrous tissue was observed at the Peri-implant of the CG material. Bone mineral apposition rate calculation, as presented in Fig. 11, showed higher in vivo mineral deposition on NG implant after 4, 8, and 12 weeks, compared to the CG counterparts.[198] The difference in the bone formation trend between NG and the CG substrates was regarded as indication of enhanced osteointegration on the bone-implant interface of the treated material.

Table 1 summarizes the recent developments toward understanding the effect of grain structure on cellular behavior, providing a brief list of the main findings based on the SPD technique, material, and cell types that were involved.

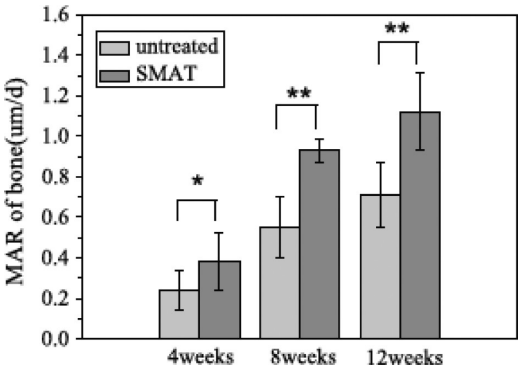

Figure 11. Bone mineral apposition rate for Ti6Al4V substrates with different grain sizes (untreated vs SMAT treated; $n = 5$, $*p > 0.05$, $**p < 0.05$) Adapted with permission from ref 198. Copyright 2010, Springer Science and Business Media.

6. DISCUSSION

Numerous implanting devices ranging from pacemakers, bone fixation (plate, screw, pin), artificial knee and hip joints, dental implants, coronary stents to spring clips for repairing large aneurysmal defects and many others are implanted in the body of ever increasing number of patients each year.[199] Considering the aging population and increasing life expectancy, utmost attention is being paid to issues correlated with the loosening and failure of metallic implants, mainly due to fatigue fracture, wear debris, poor integration, and so on. Therefore, the development of advanced multifunctional biomaterial for such applications has become a vigorously growing research area.

Nanomaterials have the significant potential to provide superior mechanical properties. Biomaterials with NG structure can be produced either through powder metallurgy or SPD techniques. The SPD methods are highly privileged compared to conventional powder metallurgy techniques because of the latter's serious drawbacks including impurity, contamination, difficulty in handling nano powders due to their high reactive nature, grain growth, and complicated sintering cycles to generate fully dense materials. Besides, SPD methods result in significant improvement of mechanical characteristics through surface and bulk grain refinement. Substantial biocompatibility and superior mechanical properties are both of essential importance to guarantee the prospective functionality and stability of the implants.

Regular articulating motions at the bearing surfaces of implant can generate wear debris. Particulate wear debris would provoke adverse biological response in joint tissues, induce inflammation and bone resorption, and eventually result in osteolysis and aseptic loosening of the implant. Periprosthetic osteolysis is known as the most common long-term complication of a total joint replacement. It is reported to result in aseptic loosening of the implant for up to 34% of younger implant recipients.[200] Hence, it seems crucial to apply approaches that can enhance the wear resistance of the implant material to assure its long-term survival and reducing the risk of revision surgeries.

More interestingly, grain refinement can provide the possibility of implementing materials that cannot be used in human body in their CG state. For instance, poor mechanical properties of Zr limit its wide application in biomedical applications regardless of its good biocompatibility. Application of SPD method to improve the mechanical properties that are directly affected by grain size can open new opportunities to its application.[175]

Another example in this field is the commercially pure Ti that is the most commonly used biomaterial in orthopedics and dentistry due to its outstanding corrosion resistance and biocompatibility.[201] Nevertheless, insufficient mechanical strength has limited the application of pure Ti in heavy loaded implants. Alloying (Ti6Al4V) has been used to enhance mechanical and biological performance of pure Ti;[196] however, there are still some issues about the cytotoxicity potentially induced by addition of aluminum and vanadium. There are numerous reports of adverse effects of the released ions on cell activities such as osteoblast metabolism and differentiation impeding the normal bone healing process.[202−204,192] Different SPD approaches that result in surface/bulk NG Ti fabrication open new possibilities for biomedical applications of pure Ti. Grain refinement enhances the mechanical properties of pure Ti, at the same time it avoids the use of the potentially toxic alloying elements.[196] Researches have been able to produce UFG pure Ti with improved strength comparable to Ti6Al4V alloy, eliminating the need to add alloying elements.[205,206] In this case SPD techniques can provide the possibility of avoiding postsurgical complications related to probable rejection of implants due to the presence of toxic elements, such as vanadium, cobalt, and nickel.[152]

Pure iron can also be recalled as another instance of application of SPD approaches to not only enhance the mechanical properties to give the possibility of using pure metals but also providing the opportunity of downsizing the medical device. In case of pure iron, grain refinement can promote the radial strength of the material and thus the thickness of the stent strut can be reduced and so does the risk of thrombosis.[165] Valiev et al. also reported the possibility of using smaller size implants after application of SPD techniques.[162,163]

Moreover, grain refinement has been reported to change the state of the surface oxide layer and consequently modulate the substrate interaction with cells. The biocompatibility of Ti based implants is mentioned to be predominantly affected by the few nm thick surface oxide layer that forms upon exposure to body fluids.[185,186] This dense passive oxide layer, characterized by its thermodynamical stability, chemical inertness, and low solubility in serum, determines the degree of surface wettability.[207] The reduced surface grain size with enhanced activity of electrons at the grain boundary junctions result in oxide protrusions, which will subsequently increase the adherence of oxide films to the substrate.[161] It is suggested that the nano porosity of this TiO_2 film mimics that of the representative ECM structures.[208] It is postulated that the state of this oxide layer and its hydrophilicity extent interferes directly with protein absorption mechanism and also the phenotype differentiation of cell.[209−211] XPS studies have confirmed that the SPD treatment does not practically change the chemical composition of the treated surface, however the thickness of the oxide layer and the structure of the crystals within it are strongly correlated with the grain structure of the material underneath.[212]

Additionally, The presence of nanosized organic and mineral phases in human bone provides the biological inspiration of using NG material for implant applications.[213] The proteins in bone ECM as well as the calcium phosphate that is a principal element of the bone are also nanostructured.[213] The NG implant surfaces are repeatedly reported to significantly alter

Table 1. Summary of Reviewed Studies on Cell−Substrate Interaction of UFG/NG Materials Produced by SPD

SPD process	cell type	substrate material	grain size	days in culture	significant findings	special features of the samples' surface
ECAP[52,53]	3T3	ASTM grade 2 pure Ti	238 nm 355 nm	in vitro 5 days	enhanced cell adhesion and proliferation on UFG samples; no significant difference in cytotoxicity	mirror finish surface
ECAP[161]	3T3	ASTM grade 2 pure Ti	240 nm	in vitro 5 days in vivo 30 days	higher fibronectin expression on UFG Ti; less macrophages in the peri- implant tissue for UFG Ti	mirror finish surface
ECAP[162,163]	L-929	ASTM grade 4 pure Ti	150 nm	in vitro 3 days	enhanced cell adhesion and colonization on UFG Ti	etched in hydrofluoric acid
ECAP[164]	MC3T3-E1	ASTM grade 2 pure Ti	200 nm	in vitro 12 days	enhanced cell viability and proliferation on UFG Ti	mirror finish surface
ECAP[165]	L-929 VSMCs ECV304	commercial pure iron	80−200 nm	in vitro 4 days	preferential cellular response in terms of viability to grain size and cell type; good hemocompatibility for all samples	smooth mechanically polished
ECAP[166]	hMSCs	ASTM Grade 2 pure Ti	170−200 nm	in vitro 2 days	accelerated cell adhesion and spreading on UFG Ti	smooth mechano-chemically polished
ECAP[168]	MG63	AZ31 magnesium alloy	8.5−1.7 μm	in vitro 3 days	acceptable toxicity to MG63 cells	
ECAP[14]	MG63	$Ni_{50.8}Ti_{49.2}$ alloy	200−300 nm	in vitro 14 days	promoted apatite forming abilities; enhanced cell attachment and proliferation	sandblasted, acid etched, alkali treated
ECAP[169]	MG63	commercial pure Ti	280 nm	in vitro 9 days	promoted apatite forming abilities and slightly enhanced cell attachment and proliferation	combined sandblasted, acid etched, alkali treated
ECAP[170]	L-929	commercial pure copper	260 ± 10 nm	in vitro 3 days	lower cytotoxicity for UFG; improved cell viability; better hemocompatibility	smooth mechanically polished
SMAT[171,172]	neonatal rat calvarial osteoblasts	Ti6Al4V	10−20 nm	in vitro 14 day	strong cellular adhesion, early cellular confluency and enhanced gene expression on NG substrate	porous surface structure
SMAT[173]	Saos-2 cells	Commercial pure Ti	25 nm	in vitro 3 days	enhanced cell adhesion, morphology, and viability	randomly rough surface (scale-like morphology)
SMAT[174]	Rat MSCs	Commercial pure Ti	40−80 nm	in vitro 21 days	improved adhesion, filament orientation, proliferation and mineralization	nanorough surface
severe rolling[175]	Saos-2 cells; (hMSC)	zirconium	240 nm	in vitro 18 days	similar cell adhesion, proliferation and mineralization on CG and UFG samples	smooth polished surface
severe rolling[177]	L-929, NIH3T3; ECV304; MG63 cell lines	SUS 304 stainless steel	50 nm	in vitro 4 days	similar cell viability on NG and CG material and good and equivalent level of cytotoxicity-free	smooth polished surface
cold rolling + phase-reversion annealing[178−180]	MC3T3-E1	316L stainless steel	<1000 nm	in vitro 7 days	enhanced cell adhesion, proliferation, viability and spread	smooth polished surface
cold rolling + phase-reversion annealing[62]	MC3T3-E1	204Cu Cr−Mn austenitic stainless steel	<1000 nm	in vitro 7 days	enhanced cell adhesion, proliferation, viability and spread	smooth polished surface
cold rolling + phase-reversion annealing[181,182]	L-929	316L stainless steel	<1000 nm	in vitro 7 days	enhanced cell adhesion, proliferation, viability and spread	smooth polished surface
cold rolling + phase-reversion annealing[183]	MC3T3-E1	301LN stainless steel	<500 nm	in vitro 5 days	positive impact of pre-adsorbed protein on cell adhesion, proliferation, and protein expression	smooth polished surface
cold rolling + phase-reversion annealing[184]	MC3T3	316L stainless steel	320 nm 538 nm 757 nm 3132 nm 22 mm	in vitro 7 days	overriding influence on cell adhesion, morphology, growth and protein expression	smooth polished surface
HPT[185,186]	MC3T3-E1; rat fibroblast Rat1 cell lines	Pure Ti	10−50 nm	in vitro 9 days	preferred adhesion of pre-osteoblasts vs. fibroblasts; enhanced cell adhesion and proliferation of pre-osteoblast and higher fibronectin expression	smooth polished surface

dx.doi.org/10.1021/am501119k | ACS Appl. Mater. Interfaces 2014, 6, 7963−7985

Table 1. continued

SPD process	cell type	substrate material	grain size	days in culture	significant findings	special features of the samples' surface
HPT[187]	L929 MG63	amorphous Ni50.2Ti49.8 Ti alloy		in vitro 4 days	similar results for cytotoxicity of L-929 and enhanced cell viability of MG63 cell lines co-cultured with extracts from NG samples	smooth polished
GP[191]	L6 cells	AZ31 magnesium alloy	5 mm	in vitro 3 days	early deposition of HA and magnesium phosphate in SBF; similar viability and better cell spreading for UFG samples	different surface roughness
ECAP[192]	MC3T3-E1	ASTM grade 2 pure Ti	200–300 nm	in vitro 7 days	enhanced cell spreading, adhesion, proliferation, ALP activity and mineralization on UFG samples	grit-blasted with HA particles
ECAP[196]	MG-63	commercial pure Ti grade 4	280 nm	in vitro 21 days	no overall change in osteoblast viability, ALP expression and proteome	smooth polished surface
ECAP[197]	L-929; MG63; VSMC; ECV304; MG63	commercial pure Ti grade 4	250 nm	in vitro 21 days in vivo 12 weeks	in vitro bioactivity and in vivo bio stability for UFG Ti	smooth polished surface
SMAT[198]	neonatal rat calvarial osteoblasts	Ti6Al4V	20–40 nm	in vitro 14 days in vivo 12 weeks	increased calcium-containing apatite formation in vitro and adjacent bone formation in vivo	randomly rough surface

the protein absorption system. The exact mechanisms that enhance cell response are not still fully clear; however, it is theorized that the interaction of certain absorbed proteins with the corresponding cell-membrane integrins may play an important role.[172]

Protein adsorption starts when the implant comes into contact with the physiological fluid, and it markedly regulates the cell substrate interaction principally cell adhesion and spreading. ECM proteins, cytoskeletal proteins, and membrane receptors (integrins) are commonly considered to interfere with cell−substrate interactions.[52] Earlier studies have extensively explored the set of proteins that are mainly involved in cell response to the substrate, such as albumin, fibronectin, vinculin, and actin, evaluating the effect of substrate grain structure on the expression and organization of such proteins and their effect on the subsequent cell response. Particularly expression of fibronectin that is among the first cell-binding proteins produced by osteoblasts and fibroblasts, also recognized as a growth simulator involved in several cell functions such as adhesion, spreading, and growth, has been evaluated.[183]

Adhesion of the cells to the substrates is considered as a fundamental step for the successive cellular activities, including spreading, proliferation, and differentiation. Indeed, a majority of the studies have focused on short-term experiments to investigate the attachment and proliferation of the cells on substrates with refined grains while there are very few studies performed on long-term response of the cell in terms of differentiation and in vivo experiments. However, it is known that the survival and proliferation rate of the cells are interconnected by the signals provided by cell adhesion through ECM.[214] Besides, the fact that grain refinement promotes cell−substrate interaction, provides the potential to eliminate the need to extra surface roughening treatments commonly used to improve cell adhesion such as sand blasting, anodizing, etching, etc.

Although there are numerous studies confirming the beneficial effect of grain refinement on protein absorption and organization,[24,178,184] there are few others reporting that such substrates do not affect the amount of protein absorption.[174,215,216]

Factors influencing adsorption of macromolecules are reported to be electrostatic, van der Waals interaction, ionic binding, and wettability.[24,185,217,218] Thus, surface chemistry, surface roughness, surface energy, and wettability are of substantial importance in this regard. The wettability is considered to have a major role in modulating the biological response of the tissues surrounding the implant.[53] Higher surface energy material exhibits higher wettability and smaller contact angle with the liquid.[161] The studies performed on protein absorption of NG substrates, have reported that enhanced surface wettability promotes protein adsorption that in turn influences the self-assembly and development of cytoskeletal proteins. Cell growth and spreading is supposed to be triggered by the arrangement and interaction of integrin receptors connecting the fibronectin to the intracellular molecules such as vinculin and actin.[184]

Misra et al.[184] reported formation of dense network of well-defined actin fibers on NG substrates as a consequence of grain size refinement relating that to the extent of surface hydrophilicity. It was concluded that surface wettability and grain structure have the ability to tune cell adhesion, spreading, viability, and their subsequent activities.

The fact that both topography and grain size contribute to alteration of surface wettability, makes it extremely challenging to determine the effect of each individual parameter. Particularly considering that majority of the studies performed in this regard have used samples with different grain size and surface topographies, the results of such investigations remain inconclusive. The very few studies that performed experiments on NG samples with similar surface topographies report the modulation of surface wettability by grain size on such samples confirming the direct effect of surface structure on hydrphilicity extent.[52,184,219]

On the other hand, there are reports focusing on effect of nanotopography of NG material on cell response, stating that the bioactivity of such material is essentially improved since the NG boundaries assemble the adsorbed proteins in a desired arrangement.[174] Increased viability of osteoblasts grown on NG substrate was mainly attributed to the nanotopography in many studies with the justification that the NG metal surfaces possess unmodified chemistry and varied surface nanotopography compared to their CG counterparts.[29] The roughness at the nanoscale is regarded to play a key role in the adsorption of proteins and consequent cell responses. Misra et al. consider the interactions between proteins and focal adhesion contacts at nanoscale responsible for activation of intracellular molecular signaling pathways.[62]

Some studies have suggested that higher density of crystalline defects and open lattice in the positions of high-angle grain boundaries provide the NG material with higher amounts of electron delocalization and consequently generate higher surface energy and electrostatic attraction, which can promote cell−substrate interaction. The higher density of open lattice and grain boundaries in UFG/NG surface are supposed to provide optimal sites for focal adhesions of cells.[182,192,220] These defects are also supposed to result in formation of focal adhesion points, which may in turn affect the process of cell signaling during cell proliferation and adhesion to the substrate.[161]

Putting all together and going through different studies performed in this filed, it can be concluded that grain refinement generally promotes various cell functions; however, some reported conflicting observations can imply the possibility of grain size as well as cell type dependent evolution of cell−substrate interaction for NG biomaterials used for metallic implants.

Studies performed to explore the effect of surface topography (in form of surface grooves and fibers) on cell adhesion have confirmed that the geometrical aspects of the grooves (width and depth) and their density on the implant surface regulate the reaction and orientation of the cells on the substrates.[221,222] It is reported that there is an optimal groove width for the cell dimension and grooves that are too wide compared to the cell dimension fail to enhance the cell activity and to induce an orientation response or cell shape alteration.[223,224] That is to say there are several reports demonstrating that cells are affected by the surface topography, while the smallest dimension that these cells may sense in early phases of interaction has not yet been accurately determined.[175] Cai et al. also report that subtle changes in surface topography of Ti films, ranging from 2 to 21 nm, do not affect the surface wettability and have no apparent effect on proliferation of human osteoblastic cells.[3] Saldana et al. report similar results of cell activities Zr substrate with different grain size. They conclude that roughness modification in nanometer scale and slight changes in the lateral distribution of topographical features below an arithmetic mean of 7 nm do not significantly alter the cell response to the substrate.[175]

In the UFG/NG material surface, such grooves are probably considerably numerous with extremely small dimensions.[52] Such a difference will apparently affect the cell response. However, considering the divergent reports, it can be postulated that different densities of the surface defects and their size on NG biomaterial can also affect the cell behavior in different ways.

Most of the reviewed studies have selected MSCs, osteoblasts and fibroblasts as object cells, with clinical rationalization that orthopedic implants would principally interact with such cells. Preferential interaction of NG substrates for different cell types such as pre-osteoblast and fibroblast and other cells was also reported in some studies.[165,185] These clear differences exhibited in cell response to the UFG/NG substrates at identical conditions indicate of a cell-type specific sensitivity to the grain structure of the substrates.

A limited number of in vivo experiments has also been performed, the results of which confirmed the improved biocompatibility of SPD treated implants; however, more detailed in vivo experiments should be carried out to shed light on the real application of SPD treated bio implants.

Another aspect that can help understanding the nature of the cell−substrate interaction in case of SPD treated material, is the mechanism that governs the mechanobiology of cell adhesion. Both experimental and computational approaches can be employed to investigate the fundamentals of how the cells feel and respond to the grain structure. Computational models, validated and supported by experimental data, can indeed prove significant insight into biological mechanisms involved in cell response to different substrates.

All in all, there seem to be a series of factors influencing the cell response to the UFG/NG SPD treated surface: higher density of surface discontinuities and nano-defects along grain boundaries, increased surface energy, higher surface wettability, and altered oxide layers state, which modulate protein absorption, cell adhesion, spreading, and the subsequent cell activities.

7. CONCLUSION AND FUTURE DEVELOPMENTS

Grain refinement obtained by severe plastic deformation processes enhances mechanical characteristics and promotes the lifetime functionality of the implant material under physiological strains. Such techniques offer the possibility of implementing materials that cannot be used in human body in their coarse grained state due to poor mechanical properties. They can help avoiding the use of expensive and potentially toxic or allergenic alloying elements; these materials can also offer the opportunity to downsize the implant or the medical device and eventually reduce the surgical intervention's consequences.

Moreover, numerous reports indicate that grain refinement can promote cell adhesion and the subsequent activities required for strong cell−substrate interaction including proliferation, differentiation, and specific developmental phenotypes expression.

Majority of the reviewed studies depict a clear grain size dependent evolution of cell−substrate interaction; however, there are still inconsistencies in the published data revealing that the biocompatibility behavior of nanostructured materials has not yet been fully understood. Indeed, experiments have

been performed on different classes of materials with a wide scatter and combination of grain size, surface topography, and cell population or animal models. This wide variety of experimental aspects makes it challenging to deconvolute biological effects of each individual factor in the eventual cell response. Although valuable insight has been already provided into effect of grain size on cell−substrate interaction, still more systematic studies are required to address the fundamental gaps in determining the mechanisms that govern the specific cell response to nanograined substrates.

The results generally suggest that dissimilar densities of the surface defects and grain size can affect cell behavior in different ways and there might be certain grain size thresholds that stimulate the mechanoreceptive responses in specific cells. Thus, future attempts should be more focused on studying the specific cell-type sensitivities to the grain structure of the substrate.

Besides, most studies have focused on evaluating short-term response of cells to such substrates and still supplementary in vivo studies are needed to validate their functionality in mediating the bone response.

To come to the point, severe plastic deformation methods promise new generation of implant materials through concurrent enhancement of mechanical characteristics and biocompatibility. These methods can particularly promote the long-lasting stability and the success rate of prosthetic rehabilitation for physio-mechanical load-bearing endosseous applications in dentistry and orthopedics. Since the obtained mechanical properties are an integral property of the material itself, and not determined by the applied severe plastic deformation technique, the choice of severe plastic deformation approach relies on its applicability to the material of interest, the average grain size that can be achieved and its potential to produce grain refinement in a continuous and economic way.

AUTHOR INFORMATION

Corresponding Authors

*Email: sbagheri@mit.edu.
*Email: alik@rics.bwh.harvard.edu.

Notes

The authors declare no competing financial interest.

ACKNOWLEDGMENTS

S.B. and R.G. acknowledge funding from MIT−Italy program (Progetto Rocca) post-doctoral fellowship.

NOMENCLATURE

SPD = severe plastic deformation
NG = nanograined
UFG = ultra fine grained
CG = coarse grained
ECAP = equal channel angular pressing
SMAT = surface mechanical attrition treatment
SSP = severe shot peening
ARB = accumulative roll bonding
HPT = high pressure torsion
GP = groove pressing
MSCs = mesenchymal stem cells
BSA = bovine serum albumin
ALP = alkaline phosphatase
SBF = simulated body fluid
HA = hydroxyapatite
ECM = extracellular matrix

REFERENCES

(1) Anselme, K.; Bigerelle, M. Statistical Demonstration of the Relative Effect of Surface Chemistry and Roughness on Human Osteoblast Short-term Adhesion. *J. Mater. Sci. Mater. Med.* **2006**, *17*, 471−479.

(2) Ward, B. C.; Webster, T. J. The Effect of Nanotopography on Calcium and Phosphorus Deposition on Metallic Materials In Vitro. *Biomaterials* **2006**, *27*, 3064−3074.

(3) Cai, K.; Bossert, J.; Jandt, K. D. Does the Nanometre Scale Topography of Titanium Influence Protein Adsorption and Cell Proliferation? *Colloids Surf., B* **2006**, *49*, 136−144.

(4) Dalby, M. J.; McCloy, D.; Robertson, M.; Agheli, H.; Sutherland, D.; Affrossman, S.; Oreffo, R. O. C. Osteoprogenitor Response to Semi-ordered and Random Nanotopographies. *Biomaterials* **2006**, *27*, 2980−2987.

(5) Khang, D.; Kim, S. Y.; Liu-Snyder, P.; Palmore, G. T. R.; Durbin, S. M.; Webster, T. J. Enhanced Fibronectin Adsorption on Carbon Nanotube/poly(carbonate) Urethane: Independent Role of Surface Nano-roughness and Associated Surface Energy. *Biomaterials* **2007**, *28*, 4756−4768.

(6) Khang, D.; Lu, J.; Yao, C.; Haberstroh, K. M.; Webster, T. J. The Role of Nanometer and Sub-micron Surface Features on Vascular and Bone Cell Adhesion on Titanium. *Biomaterials* **2008**, *29*, 970−983.

(7) Kantawong, F.; et al. Whole Proteome Analysis of Osteoprogenitor Differentiation Induced by Disordered Nanotopography and Mediated by ERK Signaling. *Biomaterials* **2009**, *30*, 4723−4731.

(8) Venkatsurya, P. K.; Thein-Han, W. W.; Misra, R. D. K.; Somani, M. C.; Karjalainen, L. P. Advancing Nanograined/ultra-fine-grained Structures for Metal Implant Technology: Interplay Between Grooving of Nano/ultra-fine-grains and Cellular Response. *Mater. Sci. Eng., C* **2010**, *30*, 1050−1059.

(9) Anselme, K.; Ponche, A.; Bigerelle, M. Relative Influence of Surface Topography and Surface Chemistry on Cell Response to Bone Implant Materials. Part 2: Biological Aspects. *Proc. Inst. Mech. Eng. H* **2010**, *224*, 1487−1507.

(10) Zhao, L.; Mei, S.; Chu, P. K.; Zhang, Y.; Wu, Z. The Influence of Hierarchical Hybrid Micro/nano-textured Titanium Surface with Titania Nanotubes on Osteoblast Functions. *Biomaterials* **2010**, *31*, 5072−5082.

(11) Rosales-Leal, J. I.; et al. Effect of Roughness, Wettability, and Morphology of Engineered Titanium Surfaces on Osteoblast-like Cell Adhesion. *Colloids Surf., A* **2010**, *365*, 222−229.

(12) Variola, F.; Brunski, J. B.; Orsini, G.; Tambasco de Oliveira, P.; Wazen, R.; Nanci, A. Nanoscale Surface Modifications of Medically Relevant Metals: State-of-the Art and Perspectives. *Nanoscale.* **2011**, *3*, 335−353.

(13) Wu, Y.; Zitelli, J. P.; TenHuisen, K. S.; Yu, X.; Libera, M. R. Differential Response of Staphylococci and Osteoblasts to Varying Titanium Surface Roughness. *Biomaterials* **2011**, *32*, 951−960.

(14) Zheng, C. Y.; Nie, F. L.; Zheng, Y. F.; Cheng, Y.; Wei, S. C.; Valiev, R. Z. Enhanced In Vitro Biocompatibility of Ultra-fine-grained Biomedical NiTi Alloy with Microporous Surface. *Appl. Surf. Sci.* **2011**, *257*, 9086−9093.

(15) Nikkhah, M.; Edalat, F.; Manoucheri, S.; Khademhosseini, A. Engineering Microscale Topographies to Control the Cell−Substrate Interface. *Biomaterials* **2012**, *33*, 5230−5246.

(16) Venkatsurya, P. K. C; Girase, B.; Misra, R. D. K.; Pesacreta, T. C.; Somani, M. C.; Karjalainen, L. P. The Interplay Between Osteoblast Functions and the Degree of Nanoscale Roughness Induced by Grain Boundary Grooving of Nanograined Materials. *Mater. Sci. Eng., C* **2012**, *32*, 330−340.

(17) Díaz, C.; Cortizo, M. C.; Schilardi, P. L.; de Saravia, S. G. G.; de Mele, M. A. F. L. Influence of The Nano−micro Structure of the Surface on Bacterial Adhesion. *Mater. Res.* **2007**, *10*, 11−14.

(18) Mitik-Dineva, N.; Wang, J.; Stoddart, P. R.; Crawford, R. J.; Ivanova, E. P. Nano-structured Surfaces Control Bacterial Attachment.

International Conference on Nanoscience and Nanotechnology. *ICONN* **2008**, 113−116.
(19) Puckett, S. D.; Taylor, E.; Raimondo, T.; Webster, T. J. The Relationship between the Nanostructure of Titanium Surfaces and Bacterial Attachment. *Biomaterials* **2010**, *31*, 706−713.
(20) Truong, V. K.; et al. The Influence of Nano-scale Surface Roughness on Bacterial Adhesion to Ultra-fine-grained Titanium. *Biomaterials* **2010**, *31*, 3674−3683.
(21) Anselme, K.; Davidson, P.; Popa, A. M.; Giazzon, M.; Liley, M.; Ploux, L. The Interaction of Cells and Bacteria with Surfaces Structured at the Nanometer Scale. *Acta Biomater.* **2010**, *6*, 3824−3846.
(22) Singh, A. V.; et al. Quantitative Characterization of the Influence of the Nanoscale Morphology of Nanostructured Surfaces on Bacterial Adhesion and Biofilm Formation. *PLoS One* **2011**, *6*, e25029.
(23) Barrett, C. S.; Massalski, T. B. *Structure of Metals*; McGraw-Hill: New York, 1966; Vol. *535*.
(24) Webster, T. J.; Ergun, C.; Doremus, R. H.; Siegel, R. W.; Bizios, R. Specific Proteins Mediate Enhanced Osteoblast Adhesion on Nanophase Ceramics. *J. Biomed. Mater. Res.* **2000**, *51*, 475−483.
(25) Valiev, R. Z.; Estrin, Y.; Horita, Z.; Langdon, T. G.; Zechetbauer, M. J.; Zhu, Y. T. Producing Bulk Ultra-fine-Grained Materials by Severe Plastic Deformation. *JOM* **2006**, *58*, 33−39.
(26) Valiev, R. Z.; Sabirov, I.; Zhilyaev, A. P.; Langdon, T. G. Bulk Nanostructured Metals for Innovative Applications. *JOM* **2012**, *64*, 1134−1142.
(27) Koch, C. C. *Nanostructured Materials Processing, Properties, and Applications*; William Andrew Pub: Norwich, NY, 2007.
(28) Langdon, T. G. Processing by Severe Plastic Deformation: Historical Developments and Current Impact. *Mater. Sci. Forum.* **2010**, *667−669*, 9−14.
(29) Webster, T. J.; Ejiofor, J. U. Increased Osteoblast Adhesion on Nanophase Metals: Ti, Ti6Al4V, and CoCrMo. *Biomaterials* **2004**, *25*, 4731−4739.
(30) Kay, S.; Thapa, A.; Haberstroh, K. M.; Webster, T. J. Nanostructured Polymer/nanophase Ceramic Composites Enhance Osteoblast and Chondrocyte Adhesion. *Tissue Eng.* **2002**, *8*, 753−761.
(31) McManus, A. J.; Doremus, R. H.; Siegel, R. W.; Bizios, R. Evaluation of Cytocompatibility and Bending Modulus of Nano-ceramic/polymer Composites. *J. Biomed. Mater. Res.* **2005**, *72A*, 98−106.
(32) Webster, T. J.; Ergun, C.; Doremus, R. H.; Siegel, R. W.; Bizios, R. Enhanced Functions of Osteoblasts on Nanophase Ceramics. *Biomaterials* **2000**, *21*, 1803−1810.
(33) Webster, T. J.; Siegel, R. W.; Bizios, R. Osteoblast Adhesion on Nanophase Ceramics. *Biomaterials* **1999**, *20*, 1221−1227.
(34) Valiev, R. Z.; Islamgaliev, R. K.; Alexandrov, I. V. *Bulk Nanostructured Materials from Severe Plastic Deformation*; Pergamon: Oxford, 2000; Vol. *45*.
(35) Meyers, M. A.; Mishra, A.; Benson, D. J. Mechanical Properties of Nanocrystalline Materials. *Prog. Mater. Sci.* **2006**, *51*, 427−556.
(36) Valiev, R. Z.; Krasilnikov, N. A.; Tsenev, N. K. Plastic Deformation of Alloys with Submicron-grained Structure. *Mater. Sci. Eng., A* **1991**, *137*, 35−40.
(37) Vinogradov, A. Y.; Stolyarov, V. V.; Hashimoto, S.; Valiev, R. Z. Cyclic Behavior of Ultra-fine-grained Titanium Produced by Severe Plastic Deformation. *Mater. Sci. Eng., A* **2001**, *318*, 163−173.
(38) Yamashita, A.; Horita, Z.; Langdon, T. G. Improving the Mechanical Properties of Magnesium and a Magnesium Alloy Through Severe Plastic Deformation. *Mater. Sci. Eng., A* **2001**, *300*, 142−147.
(39) Rybal'chenko, O. V.; Dobatkin, S. V.; Kaputkina, L. M.; Raab, G. I.; Krasilnikov, N. A. Strength of Ultra-fine-grained Corrosion-Resistant Steels After Severe Plastic Deformation. *Mater. Sci. Eng., A* **2004**, *387−389*, 244−248.
(40) Mishra, A.; Kad, B.; Gregori, F.; Meyers, M. Microstructural Evolution in Copper Subjected to Severe Plastic Deformation: Experiments and Analysis. *Acta Mater.* **2007**, *55*, 13−28.
(41) Bagheri, S.; Guagliano, M. Review of Shot Peening Processes to Obtain Nanocrystalline Surfaces in Metal Alloys. *Surf. Eng.* **2009**, *25*, 3−14.
(42) Estrin, Y.; Vinogradov, A. Fatigue Behavior of Light Alloys with Ultra-fine-grain Structure Produced by Severe Plastic Deformation: An Overview. *Int. J. Fatigue.* **2010**, *32*, 898−907.
(43) Ortiz-Cuellar, E.; Hernandez-Rodriguez, M. A. L.; García-Sanchez, E. Evaluation of the Tribological Properties of an Al−Mg−Si Alloy Processed by Severe Plastic Deformation. *Wear* **2011**, *271*, 1828−1832.
(44) Bagherifard, S.; Guagliano, M. Fatigue Behavior of a Low-alloy Steel with Nanostructured Surface Obtained by Severe Shot Peening. *Eng. Fract. Mech.* **2012**, *81*, 56−68.
(45) Djavanroodi, F.; Daneshtalab, M.; Ebrahimi, M. A Novel Technique to Increase Strain Distribution Homogeneity for ECAPed Materials. *Mater. Sci. Eng., A* **2012**, *535*, 115−121.
(46) Sajadi, A.; Ebrahimi, M.; Djavanroodi, F. Experimental and Numerical Investigation of Al Properties Fabricated by CGP Process. *Mater. Sci. Eng., A* **2012**, *552*, 97−103.
(47) Estrin, Y.; Vinogradov, A. Extreme Grain Refinement by Severe Plastic Deformation: A Wealth of Challenging Science. *Acta Mater.* **2013**, *61*, 782−817.
(48) Bagherifard, S.; Fernandez-Pariente, I.; Ghelichi, R.; Guagliano, M. Fatigue Behavior of Notched Steel Specimens with Nanocrystallized Surface Obtained by Severe Shot Peening. *Mater. Des.* **2013**, *45*, 497−503.
(49) Miková, K.; Bagherifard, S.; Bokuvka, O.; Guagliano, M.; Trško, L. Fatigue Behavior of X70 Microalloyed Steel After Severe Shot Peening. *Int. J. Fatigue* **2013**, *55*, 33−42.
(50) Ghelichi, R.; Bagherifard, S.; Mac Donald, D.; Brochu, M.; Jahed, H.; Jodoin, B.; Guagliano, M. Fatigue Strength of Al Alloy Cold Sprayed with Nanocrystalline Powders. *Int. J. Fatigue* **2013**, DOI: 10.1016/j.ijfatigue.2013.09.001.
(51) Bagherifard, S.; Fernandez-Pariente, I.; Ghelichi, R.; Guagliano, M. Effect of Severe Shot Peening on Microstructure and Fatigue Strength of Cast Iron. *Int. J. Fatigue* **2013**, DOI: 10.1016/j.ijfatigue.2013.08.022.
(52) Kim, T. N.; Balakrishnan, A.; Lee, B. C.; Kim, W. S.; Smetana, K.; Park, J. K.; Panigrahi, B. B. In Vitro Biocompatibility of Equal Channel Angular Processed (ECAP) Titanium. *Biomed. Mater.* **2007**, *2*, S117−S120.
(53) Kim, T. N.; et al. In Vitro Fibroblast Response to Ultra-fine-grained Titanium Produced by a Severe Plastic Deformation Process. *J. Mater. Sci.: Mater. Med.* **2007**, *19*, 553−557.
(54) Webster, T. J.; Siegel, R. W.; Bizios, R. Design and Evaluation of Nanophase Alumina for Orthopaedic/Dental Applications. *NanoStruct. Mater.* **1999**, *12*, 983−986.
(55) Sato, M.; Sambito, M. A.; Aslani, A.; Kalkhoran, N. M.; Slamovich, E. B.; Webster, T. J. Increased Osteoblast Functions on Undoped and Yttrium-doped Nanocrystalline Hydroxyapatite Coatings on Titanium. *Biomaterials* **2006**, *27*, 2358−2369.
(56) Balasundaram, G.; Webster, T. J. A Perspective on Nanophase Materials for Orthopedic Implant Applications. *J. Mater. Chem.* **2006**, *16*, 3737−3745.
(57) Ward, B. C.; Webster, T. J. Increased Functions of Osteoblasts on Nanophase Metals. *Mater. Sci. Eng., C* **2007**, *27*, 575−578.
(58) Lin, C. C.; Cheng, H. C.; Huang, C. F.; Lin, C. T.; Lee, S. Y.; Chen, C. S.; Ou, K. L. Enhancement of Biocompatibility on Bioactive Titanium Surface by Low-Temperature Plasma Treatment. *Jpn. J. Appl. Phys.* **2005**, *44*, 8590−8598.
(59) Geetha, M.; Singh, A.K.; Asokamani, R.; Gogia, A.K. Ti Based Biomaterials, the Ultimate Choice for Orthopaedic Implants—A Review. *Prog. Mater. Sci.* **2009**, *54*, 397−425.
(60) Fowkes, F. M.; Gould, R. F.; Eds. *Contact Angle, Wettability, and Adhesion*; Advances in Chemistry Series; American Chemical Society: Washington, DC, 1964; Vol. *43*.
(61) Fecht, H. J. Nanophase Materials by Mechanical Attrition: Synthesis and Characterization. In *Nanophase Materials*; Hadjipanayis, G. C.; Siegel, R. W., Eds.; Springer: Netherlands, 1994; pp 125−144.

(62) Misra, R. D. K.; Girase, B.; Venkata Surya, P. K. C.; Somani, M. C.; Karjalainen, L. P. Cellular Mechanisms of Enhanced Osteoblasts Functions via Phase-Reversion Induced Nano/Submicron-grained Structure in a Low-Ni Austenitic Stainless Steel. *Adv. Eng. Mater.* **2011**, *13*, B483−B492.
(63) Valiev, R. Nanostructuring of Metals by Severe Plastic Deformation for Advanced Properties. *Nat. Mater.* **2004**, *3*, 511−516.
(64) Valiev, R. Z.; Langdon, T. G. Principles of Equal-channel Angular Pressing as a Processing Tool for Grain Refinement. *Prog. Mater. Sci.* **2006**, *51*, 881−981.
(65) Stolyarov, V. V.; Zhu, Y. T.; Alexandrov, I. V.; Lowe, T. C.; Valiev, R. Z. Influence of ECAP Routes on the Microstructure and Properties of Pure Ti. *Mater. Sci. Eng., A* **2001**, *299*, 59−67.
(66) Shin, D.; Kim, I.; Kim, J.; Kim, Y.; Semiatin, S. Microstructure Development During Equal-Channel Angular Pressing of Titanium. *Acta Mater.* **2003**, *51*, 983−996.
(67) Skrotzki, W.; Tóth, L. S.; Klöden, B.; Brokmeier, H. G.; Arruffat-Massion, R. Texture After ECAP of a Cube-Oriented Ni Single Crystal. *Acta Mater.* **2008**, *56*, 3439−3449.
(68) Xu, C.; Schroeder, S.; Berbon, P. B.; Langdon, T. G. Principles of ECAP−Conform as a Continuous Process for Achieving Grain Refinement: Application to an Aluminum Alloy. *Acta Mater.* **2010**, *58*, 1379−1386.
(69) Mckenzie, P. W. J; Lapovok, R.; Estrin, Y. The Influence of Back Pressure on ECAP Processed AA 6016, Modeling and Experiment. *Acta Mater.* **2007**, *55*, 2985−2993.
(70) Qian, T.; Marx, M.; Schüler, K.; Hockauf, M.; Vehoff, H. Plastic Deformation Mechanism of Ultra-Fine-Grained AA6063 Processed by Equal-Channel Angular Pressing. *Acta Mater.* **2012**, *58*, 2112−2123.
(71) Kim, W.; Sa, Y. Micro-extrusion of ECAP Processed Magnesium Alloy for Production of High Strength Magnesium Micro-gears. *Scr. Mater.* **2006**, *54*, 1391−1395.
(72) Kim, W. J.; Chung, C. S.; Ma, D. S.; Hong, S. I.; Kim, H. K. Optimization of Strength and Ductility of 2024 Al by Equal Channel Angular Pressing (ECAP) and Post-ECAP Aging. *Scr. Mater.* **2003**, *49*, 333−338.
(73) Liu, T.; Wang, Y. D.; Wu, S. D.; Lin Peng, R.; Huang, C. X.; Jiang, C. B.; Li, S. X. Textures and Mechanical Behavior of Mg−3.3%Li Alloy After ECAP. *Scr. Mater.* **2004**, *51*, 1057−1061.
(74) Kim, J. K.; Kim, H. K.; Park, J. W.; Kim, W. J. Large Enhancement in Mechanical Properties of the 6061 Al Alloys After a Single Pressing by ECAP. *Scr. Mater.* **2005**, *53*, 1207−1211.
(75) Mckenzie, P. W. J.; Lapovok, R. ECAP with Back Pressure for Optimum Strength and Ductility in Aluminium Alloy 6016. Part 1: Microstructure. *Acta Mater.* **2010**, *58*, 3198−3211.
(76) Cardoso, K. R.; Travessa, D. N.; Botta, W. J.; Jorge, A. M. High Strength AA7050 Al Alloy Processed by ECAP: Microstructure and Mechanical Properties. *Mater. Sci. Eng., A* **2011**, *528*, 5804−5811.
(77) del Valle, J. A.; Carreño, F.; Ruano, O. A. Influence of Texture and Grain Size on Work Hardening and Ductility in Magnesium-Based Alloys Processed by ECAP and Rolling. *Acta Mater.* **2006**, *54*, 4247−4259.
(78) Sabirov, I.; Estrin, Y.; Barnett, M.R.; Timokhina, I.; Hodgson, P.D. Enhanced Tensile Ductility of an Ultra-fine-grained Aluminum Alloy. *Scr. Mater.* **2008**, *58*, 163−16.
(79) Valiev, R. Z.; Islamgaliev, R. K.; Semenova, I. P. Superplasticity in Nanostructured Materials: New Challenges. *Mater. Sci. Eng., A* **2007**, *463*, 2−7.
(80) Mahmudi, R.; Alizadeh, R.; Geranmayeh, A. R. Enhanced superplasticity in equal-channel angularly pressed Sn−5Sb alloy. *Scr. Mater.* **2011**, *64*, 521−524.
(81) Balyanov, A. Corrosion Resistance of Ultra Fine-Grained Ti. *Scr. Mater.* **2004**, *51*, 225−229.
(82) Abd El Aal, M. I.; El Mahallawy, N.; Shehata, F. A.; Abd El Hameed, M.; Yoon, E. Y.; Kim, H.S. Wear Properties of ECAP-Processed Ultra-fine-grained Al−Cu Alloys. *Mater. Sci. Eng. A* **2010**, *527*, 3726−3732.
(83) Ma, A.; Suzuki, K.; Saito, N.; Nishida, Y.; Takagi, M.; Shigematsu, I.; Iwata, H. Impact Toughness of an Ingot Hypereutectic Al−23mass% Si Alloy Improved by Rotary-Die Equal-Channel Angular Pressing. *Mater. Sci. Eng. A* **2006**, *399*, 181−189.
(84) Singh, A.; Tang, L.; Dao, M.; Lu, L.; Suresh, S. Fracture Toughness and Fatigue Crack Growth Characteristics of Nanotwinned Copper. *Acta Mater.* **2011**, *59*, 2437−2446.
(85) Ueno, H.; Kakihata, K.; Kaneko, Y.; Hashimoto, S.; Vinogradov, A. Enhanced Fatigue Properties of Nanostructured Austenitic SUS 316L Stainless Steel. *Acta Mater.* **2011**, *59*, 7060−7069.
(86) Li, R. H.; Zhang, Z. J.; Zhang, P.; Zhang, Z. F. Improved Fatigue Properties of Ultra-fine-grained Copper Under Cyclic Torsion Loading. *Acta Mater.* **2013**, *61*, 5857−5868.
(87) Soliman, M. S.; El-Danaf, E. A.; Almajid, A. A. Enhancement of Static and Fatigue Strength of 1050 Al Processed by Equal-Channel Angular Pressing Using Two Routes. *Mater. Sci. Eng. A* **2012**, *532*, 120−129.
(88) Stolyarov, V. V.; Shuster, L. S.; Migranov, M. S.; Valiev, R. Z.; Zhu, Y. T. Reduction of Friction Coefficient of Ultra-fine-grained CP Titanium. *Mater. Sci. Eng. A* **2004**, *371*, 313−317.
(89) Zhu, Y. T.; Lowe, T. C.; Valiev, R. Z.; Stolyarov, V. V.; Latysh, V. V.; Raab, G. J. *Ultra-fine-grained Titanium for Medical Implants*. U.S. Patent No. US6399215 B1, June, 4, 2002.
(90) Lu, K.; Lu, J. Surface Nanocrystallization (SNC) of Metallic Materials-Presentation of the Concept Behind a New Approach. *J. Mater. Sci. Technol.* **1999**, *15*, 193−197.
(91) Tao, N. R.; Sui, M. L.; Lu, J.; Lu, K. Surface Nanocrystallization of Iron Induced by Ultrasonic Shot Peening. *Nanostruct.Mater.* **1999**, *11*, 433−440.
(92) Tao, N. R.; Wang, Z. B.; Tong, W. P.; Sui, M. L.; Lu, J.; Lu, K. An Investigation of Surface Nanocrystallization Mechanism in Fe Induced by Surface Mechanical Attrition Treatment. *Acta Mater.* **2002**, *50*, 4603−4616.
(93) Zhang, H.; Hei, Z.; Liu, G.; Lu, J.; Lu, K. Formation of Nanostructured Surface Layer on AISI 304 Stainless Steel by Means of Surface Mechanical Attrition Treatment. *Acta Mater.* **2003**, *51*, 1871−1881.
(94) Zhu, K. Y.; Vassel, A.; Brisset, F.; Lu, K.; Lu, J. Nanostructure Formation Mechanism of α-Titanium Using SMAT. *Acta Mater.* **2004**, *52*, 4101−4110.
(95) Liu, Z. G.; Fecht, H. J.; Umemoto, M. Microstructural Evolution and Nanocrystal Formation During Deformation of Fe−C Alloys. *Mater. Sci. Eng. A* **2004**, *375−377*, 839−843.
(96) Wu, X.; Tao, N.; Hong, Y.; Xu, B.; Lu, J.; Lu, K. Microstructure and Evolution of Mechanically-Induced Ultra-fine-grained in Surface Layer of AL-Alloy Subjected to USSP. *Acta Mater.* **2002**, *50*, 2075−2084.
(97) Lu, K.; Lu, J. Nanostructured Surface Layer on Metallic Materials Induced by Surface Mechanical Attrition Treatment. *Mater. Sci. Eng. A* **2004**, *375−377*, 38−45.
(98) Ren, J.; Shan, A.; Zhang, J.; Song, H.; Liu, J. Surface Nanocrystallization of Ni_3Al by Surface Mechanical Attrition Treatment. *Mater. Lett.* **2006**, *60*, 2076−2079.
(99) Arif, B.; Vianto, S.; Mahardika, M.; Dewo, P.; Iswanto, P. T.; Salim, U. A. Effect of Surface Mechanical Attrition Treatment (SMAT) on Microhardness, Surface Roughness and Wettability of AISI 316L. *Mater. Chem. Phys.* **2011**, *125*, 418−426.
(100) Lü, A. Q.; Zhang, Y.; Li, Y.; Liu, G.; Zang, Q. H.; Liu, C. M. Effect of Nanocrystalline and Twin Boundaries on Corrosion Behavior ot 316L Stainless Steel Using SMAT. *Acta Metall. Sin. (Engl. Lett.)* **2006**, *19*, 183−189.
(101) Huang, R.; Han, Y. The Effect of SMAT-induced Grain Refinement and Dislocations on the Corrosion Behavior of Ti−25Nb−3Mo−3Zr−2Sn Alloy. *Mater. Sci. Eng., C* **2013**, *33*, 2353−2359.
(102) Jelliti, S.; Richard, C.; Retraint, D.; Roland, T.; Chemkhi, M.; Demangel, C. Effect of Surface Nanocrystallization on the Corrosion Behavior of Ti−6Al−4V Titanium Alloy. *Surf. Coat. Technol.* **2013**, *224*, 82−87.
(103) Roland, T.; Retraint, D.; Lu, K.; Lu, J. Fatigue Life Improvement Through Surface Nanostructuring of Stainless Steel by

Means of Surface Mechanical Attrition Treatment. *Scr. Mater.* **2006**, *54*, 1949−1954.
(104) Li, D.; Chen, H. N.; Xu, H. The Effect of Nanostructured Surface Layer on the Fatigue Behaviors of a Carbon Steel. *Appl. Surf. Sci.* **2009**, *255*, 3811−3816.
(105) Tong, W. P. Nitriding Iron at Lower Temperatures. *Science* **2003**, *299*, 686−688.
(106) Tong, W. P.; Liu, C. Z.; Wang, W.; Tao, N. R.; Wang, Z. B.; Zuo, L.; He, J. C. Gaseous Nitriding of Iron with a Nanostructured Surface Layer. *Scr. Mater.* **2007**, *57*, 533−536.
(107) Lin, Y.; Lu, J.; Wang, L.; Xu, T.; Xue, Q. Surface Nanocrystallization by Surface Mechanical Attrition Treatment and its Effect on Structure and Properties of Plasma Nitrided AISI 321 Stainless Steel. *Acta Mater.* **2006**, *54*, 5599−5605.
(108) Saha, R.; Ray, R. K. Formation of Nano- to Ultra-fine-grains in a Severely Cold Rolled Interstitial Free Steel. *Mater. Sci. Eng. A* **2007**, *459*, 223−226.
(109) Hallberg, H. Influence of Process Parameters on Grain Refinement in AA1050 Aluminum During Cold Rolling. *Int. J. Mech. Sci.* **2013**, *66*, 260−272.
(110) Saito, Y.; Utsunomiya, H.; Tsuji, N.; Sakai, T. Novel Ultra-high Straining Process for Bulk Materials—Development of the Accumulative Roll-Bonding (ARB) Process. *Acta Mater.* **1999**, *47*, 579−583.
(111) Costa, A. L. M.; Reis, A. C. C.; Kestens, L.; Andrade, M. S. Ultra-grain Refinement and Hardening of IF-Steel during Accumulative Roll-Bonding. *Mater. Sci. Eng. A* **2005**, *406*, 279−285.
(112) Kim, W. J.; Lee, K. E.; Choi, S. H. Mechanical Properties and Microstructure of Ultra-fine-grained Copper Prepared by a High-Speed-Ratio Differential Speed Rolling. *Mater. Sci. Eng. A* **2009**, *506*, 71−79.
(113) Kim, W. J.; Yoo, S. J.; Lee, J. B. Microstructure and Mechanical Properties of Pure Ti Processed by High-Ratio Differential Speed Rolling at Room Temperature. *Scr. Mater.* **2010**, *62*, 451−454.
(114) Kim, W. J.; Wang, J. Y.; Choi, S. O.; Choi, H. J.; Sohn, H. T. Synthesis of Ultra-high Strength Al−Mg−Si Alloy Sheets by Differential Speed Rolling. *Mater. Sci. Eng. A* **2009**, *520*, 23−28.
(115) Müller, A.; Garcés, G.; Pérez, P.; Adeva, P. Grain Refinement of Mg−Zn−Y Alloy Reinforced by an Icosahedral Quasicrystalline Phase by Severe Hot Rolling. *J. Alloys Compd.* **2007**, *443*, L1−L5.
(116) Hosseini, S. A.; Manesh, H. D. High-strength, High-Conductivity Ultra-fine-grains Commercial Pure Copper Produced by ARB Process. *Mater. Des.* **2009**, *30*, 2911−2918.
(117) Wang, J.; Xu, R.; Wang, S.; Qian, T.; Shi, Q. Formation Mechanism and Organizational Controlling of Ultra-fine-grain Copper Processed by Asymmetrical Accumulative Rolling-Bond and Annealing. *Trans. Nonferrous Met. Soc. China* **2012**, *22*, 2672−2678.
(118) Wang, D.; Ma, Z. Y.; Gao, Z. M. Effects of Severe Cold Rolling on Tensile Properties and Stress Corrosion Cracking of 7050 Aluminum Alloy. *Mater. Chem. Phys.* **2009**, *117*, 228−233.
(119) Tomimura, K.; Takaki, S.; Tokunaga, Y. Reversion Mechanism from Deformation Induced Martensite to Austenite in Metastable Austenitic Stainless-Steels. *Isij Int.* **1991**, *31*, 1431−1437.
(120) Tomimura, K.; Nagamori, H.; Takaki, S.; Tokunaga, Y. Tensile Deformation-Behavior in Metastable Austenitic Stainless-Steel Having Ultra Fine-Grain Structure. *J. Jpn. Inst. Met.* **1991**, *55*, 376−382.
(121) Tomimura, K.; Kawauchi, Y.; Takaki, S.; Tokunaga, Y. Effect of Prior Deformation on Grain Refining Process of Martensitic Shear Reversion in Metastable Austenitic Stainless-Steel. *Tetsu Hagane—J. Iron Steel Inst. Jpn.* **1991**, *77*, 1519−1526.
(122) Misra, R. D. K.; Kumar, B. R.; Somani, M.; Karjalainen, P. Deformation Processes During Tensile Straining of Ultra-fine/Nanograined Structures Formed by Reversion in Metastable Austenitic Steels. *Scr. Mater.* **2008**, *59*, 79−82.
(123) Schino, A. D.; Barteri, M.; Kenny, J. M. Development of Ultra Fine Grain Structure by Martensitic Reversion in Stainless Steel. *J. Mater. Sci. Lett.* **2002**, *21*, 751−753.
(124) Tsuchiyama, T.; Nakamura, Y.; Hidaka, H.; Takaki, S. Effect of Initial Microstructure on Superplasticity in Ultra-fine-grained 18 Cr-9 Ni Stainless Steel. *Mater. Trans.* **2004**, *45*, 2259−2263.
(125) Jin, J. E.; Jung, Y. S.; Lee, Y. K. Effect of Grain Size on the Uniform Ductility of a Bulk Ultra-fine-grained Alloy. *Mater. Sci. Eng. A* **2007**, *449−451*, 786−789.
(126) Hamada, A. S.; Karjalainen, L. P.; Somani, M. C. Electrochemical Corrosion Behavior of a Novel Submicron-grained Austenitic Stainless Steel in an Acidic NaCl Solution. *Mater. Sci. Eng. A* **2006**, *431*, 211−217.
(127) Smirnova, N.; Levit, V.; Pilyugin, V.; Kuznetsov, R.; Davydova, L.; Sazonova, V. Evolution of the Fcc Single-Crystal Structure During Severe Plastic-Deformations. *Fiz. Met. Metalloved.* **1986**, *61*, 1170−1177.
(128) Valiev, R. Z.; Ivanisenko, Y. V.; Rauch, E. F.; Baudelet, B. Structure and Deformaton Behavior of Armco Iron Subjected to Severe Plastic Deformation. *Acta Mater.* **1996**, *44*, 4705−4712.
(129) Zhilyaev, A.; Langdon, T. Using High-Pressure Torsion for Metal Processing: Fundamentals and Applications. *Prog. Mater. Sci.* **2008**, *53*, 893−979.
(130) Zhilyaev, A.; Nurislamova, G.; Kim, B. K.; Baró, M.; Szpunar, J.; Langdon, T. Experimental Parameters Influencing Grain Refinement and Microstructural Evolution During High-Pressure Torsion. *Acta Mater.* **2003**, *51*, 753−765.
(131) Sergueeva, A. V.; Stolyarov, V. V.; Valiev, R. Z.; Mukherjee, A. K. Advanced Mechanical Properties of Pure Titanium with Ultra-fine-grained Structure. *Scr. Mater.* **2001**, *45*, 747−752.
(132) Valiev, R. Z.; Mukherjee, A. K. Nanostructures and Unique Properties in Intermetallics, Subjected to Severe Plastic Deformation. *Scr. Mater.* **2001**, *44*, 1747−1750.
(133) Wei, Q.; et al. Microstructure and Mechanical Properties of Super-Strong Nanocrystalline Tungsten Processed by High-Pressure Torsion. *Acta Mater.* **2006**, *54*, 4079−4089.
(134) Tian, Y. Z.; Wu, S. D.; Zhang, Z. F.; Figueiredo, R. B.; Gao, N.; Langdon, T. G. Microstructural Evolution and Mechanical Properties of a Two-Phase Cu−Ag Alloy Processed by High-Pressure Torsion to Ultrahigh Strains. *Acta Mater.* **2011**, *59*, 2783−2796.
(135) Jóni, B.; Schafler, E.; Zehetbauer, M.; Tichy, G.; Ungár, T. Correlation Between the Microstructure Studied by X-ray Line Profile Analysis and the Strength of High-Pressure-Torsion Processed Nb and Ta. *Acta Mater.* **2013**, *61*, 632−642.
(136) McFadden, S. X.; Mishra, R. S.; Valiev, R. Z.; Zhilyaev, A. P.; Mukherjee, A. K. Low-Temperature Superplasticity in Nanostructured Nickel and Metal Alloys. *Nature* **1999**, *398*, 684−686.
(137) Valiev, R. Materials Science: Nanomaterial Advantage. *Nature* **2002**, *419*, 887−889.
(138) Turba, K.; Málek, P.; Cieslar, M. Superplasticity in an Al−Mg−Zr−Sc Alloy Produced by Equal-Channel Angular Pressing. *Mater. Sci. Eng. A* **2007**, *462*, 91−94.
(139) Furukawa, M.; Horita, Z.; Nemoto, M.; Valiev, R. Z.; Langdon, T. G. Microhardness Measurements and the Hall−Petch Relationship in an Al Mg Alloy with Submicrometer Grain Size. *Acta Mater.* **1996**, *44*, 4619−4629.
(140) Horita, Z.; Langdon, T. G. Microstructures and Microhardness of an Aluminum Alloy and Pure Copper after Processing by High-Pressure Torsion. *Mater. Sci. Eng. A* **2005**, *410−411*, 422−425.
(141) Wei, Q.; Pan, Z. L.; Wu, X. L.; Schuster, B. E.; Kecskes, L. J.; Valiev, R. Z. Microstructure and Mechanical Properties at Different Length Scales and Strain Rates of Nanocrystalline Tantalum Produced by High-Pressure Torsion. *Acta Mater.* **2011**, *59*, 2423−2436.
(142) Starink, M. J.; Cheng, X.; Yang, S. Hardening of Pure Metals by High-Pressure Torsion: A Physically Based Model Employing Volume-Averaged Defect Evolutions. *Acta Mater.* **2013**, *61*, 183−192.
(143) Khatibi, G.; Horky, J.; Weiss, B.; Zehetbauer, M. J. High Cycle Fatigue Behavior of Copper Deformed by High Pressure Torsion. *Int. J. Fatigue.* **2010**, *32*, 269−278.
(144) Horky, J.; Khatibi, G.; Weiss, B.; Zehetbauer, M. J. Role of Structural Parameters of Ultra-fine-grained Cu for its Fatigue and Crack Growth Behavior. *J. Alloys Compd.* **2011**, *509*, S323−S327.
(145) Gao, J. H.; Guan, S.K.; Ren, Z. W.; Sun, Y. F.; Zhu, S. J.; Wang, B. Homogeneous Corrosion of High Pressure Torsion Treated Mg−

Zn−Ca Alloy in Simulated Body Fluid. *Mater. Lett.* **2011**, *65*, 691−693.
(146) Rogl, G.; et al. High-Pressure Torsion, a New Processing Route for Thermoelectrics of High ZTs by Means of Severe Plastic Deformation. *Acta Mater.* **2012**, *60*, 2146−2157.
(147) Shin, D. H.; Park, J. J.; Kim, Y.S.; Park, K. T. Constrained Groove Pressing and Its Application to Grain Refinement of Aluminum. *Mater. Sci. Eng. A* **2002**, *328*, 98−103.
(148) Lee, J.; Park, J. Numerical and Experimental Investigations of Constrained Groove Pressing and Rolling for Grain Refinement. *J. Mater. Process. Technol.* **2002**, *130−131*, 208−213.
(149) Peng, K.; Zhang, Y.; Shaw, L. L.; Qian, K. W. Microstructure Dependence of a Cu−38Zn Alloy on Processing Conditions of Constrained Groove Pressing. *Acta Mater.* **2009**, *57*, 5543−5553.
(150) Satheesh Kumar, S. S.; Raghu, T. Mechanical Behavior and Microstructural Evolution of Constrained Groove Pressed Nickel Sheets. *J. Mater. Process. Technol.* **2013**, *213*, 214−220.
(151) Krishnaiah, A.; Chakkingal, U.; Venugopal, P. Production of Ultrafine Grain Sizes in Aluminium Sheets by Severe Plastic Deformation Using the Technique of Groove Pressing. *Scr. Mater.* **2005**, *52*, 1229−1233.
(152) Peng, K.; Su, L.; Shaw, L.; Qian, K. Grain Refinement and Crack Prevention in Constrained Groove Pressing of Two-Phase Cu−Zn Alloys. *Scr. Mater.* **2007**, *56*, 987−990.
(153) Satheesh Kumar, S. S.; Raghu, T. Tensile Behavior and Strain Hardening Characteristics of Constrained Groove Pressed Nickel Sheets. *Mater. Des.* **2011**, *32*, 4650−4657.
(154) Morattab, S.; Ranjbar, K.; Reihanian, M. On the Mechanical Properties and Microstructure of Commercially Pure Al Fabricated by Semi-constrained Groove Pressing. *Mater. Sci. Eng. A* **2011**, *528*, 6912−6918.
(155) Niranjan, G. G.; Chakkingal, U. Deep Drawability of Commercial Purity Aluminum Sheets Processed by Groove Pressing. *J. Mater. Process. Technol.* **2010**, *210*, 1511−1516.
(156) Khodabakhshi, F.; Kazeminezhad, M. The Annealing Phenomena and Thermal Stability of Severely Deformed Steel Sheet. *Mater. Sci. Eng. A* **2011**, *528*, 5212−5218.
(157) Sarkari Khorrami, M.; Kazeminezhad, M.; Kokabi, A. H. Thermal Stability During Annealing of Friction Stir Welded Aluminum Sheet Produced by Constrained Groove Pressing. *Mater. Des.* **2013**, *45*, 222−227.
(158) Khodabakhshi, F.; Kazeminezhad, M. The Effect of Constrained Groove Pressing on Grain Size, Dislocation Density, and Electrical Resistivity of Low Carbon Steel. *Mater. Des.* **2011**, *32*, 3280−3286.
(159) Mosmann, T. Rapid Colorimetric Assay for Cellular Growth and Survival: Application to Proliferation and Cytotoxicity Assays. *J. Immunol. Methods.* **1983**, *65*, 55−63.
(160) Ferrari, M.; Fornasiero, M. C.; Isetta, A.M. MTT Colorimetric Assay for Testing Macrophage Cytotoxic Activity In Vitro. *J. Immunol. Methods.* **1990**, *131*, 165−172.
(161) Bindu, S.; Sanosh, K. P.; Smetana, K.; Balakrishnan, A.; Kim, T. N. An In Vivo Evaluation of Ultra-fine-grained Titanium Implants. *J. Mater. Sci. Technol.* **2009**, *25*, 556−560.
(162) Valiev, R. Z.; et al. Nanostructured SPD Processed Titanium for Medical Implants. *Materials Science Forum* **2008**, *584*, 49−54.
(163) Valiev, R. Z.; Semenova, I. P.; Latysh, V. V.; Shcherbakov, A. V.; Yakushina, E. B. Nanostructured Titanium for Biomedical Applications: New Developments and Challenges for Commercialization. *Nanotechnologies Russ.* **2008**, *3*, 593−601.
(164) Estrin, Y.; Kasper, C.; Diederichs, S.; Lapovok, R. Accelerated Growth of Preosteoblastic Cells on Ultra-fine-grained Titanium. *J. Biomed. Mater. Res. Part A* **2009**, *90A*, 1239−1242.
(165) Nie, F. L.; Zheng, Y. F.; Wei, S. C.; Hu, C.; Yang, G. In Vitro Corrosion, Cytotoxicity, and Hemocompatibility of Bulk Nanocrystalline Pure Iron. *Biomed. Mater.* **2010**, *5*, 065015.
(166) Estrin, Y.; Ivanova, E. P.; Michalska, A.; Truong, V. K.; Lapovok, R.; Boyd, R. Accelerated Stem Cell Attachment to Ultra-fine-grained Titanium. *Acta Biomater.* **2011**, *7*, 900−906.
(167) Li, Z.; Gu, X.; Lou, S.; Zheng, Y. The Development of Binary Mg−Ca Alloys for Use as Biodegradable Materials within Bone. *Biomaterials* **2008**, *29*, 1329−1344.
(168) Gu, X. N.; Li, N.; Zheng, Y. F.; Kang, F.; Wang, J. T.; Ruan, L. In Vitro Study on Equal Channel Angular Pressing AZ31 Magnesium Alloy with and without Back Pressure. *Mater. Sci. Eng. B* **2011**, *176*, 1802−1806.
(169) Zheng, C. Y.; Nie, F. L.; Zheng, Y. F.; Cheng, Y.; Wei, S. C.; Valiev, R. Z. Enhanced In Vitro Biocompatibility of Ultrafine-Grained Titanium with Hierarchical Porous Surface. *Appl. Surf. Sci.* **2011**, *257*, 5634−5640.
(170) Xu, X. X.; Nie, F. L.; Wang, Y. B.; Zhang, J. X.; Zheng, W.; Li, L.; Zheng, Y. F. Effective Inhibition of the Early Copper Ion Burst Release with Ultra-fine-grained Copper and Single Crystal Copper for Intrauterine Device Application. *Acta Biomater.* **2012**, *8*, 886−896.
(171) Ji, W.; Han, P.; Zhao, C.; Jiang, Y.; Zhang, X. Increased Osteoblast Adhesion on Nanophase Ti6Al4V. *Chin. Sci. Bull.* **2008**, *53*, 1757−1762.
(172) Han, P.; Ji, W.; Zhao, C.; Zhang, X.; Jiang, Y. Improved Osteoblast Proliferation, Differentiation and Mineralization on Nanophase Ti6Al4V. *Chin. Med. J. (Beijing, China, Engl. Ed.)* **2011**, *124*, 273−279.
(173) Zhao, C.; Han, P.; Ji, W.; Zhang, X. Enhanced Mechanical Properties and in Vitro Cell Response of Surface Mechanical Attrition Treated Pure Titanium. *J. Biomater. Appl.* **2011**, *27*, 113−118.
(174) Lai, M.; Cai, K.; Hu, Y.; Yang, X.; Liu, Q. Regulation of the Behaviors of Mesenchymal Stem Cells by Surface Nanostructured Titanium. *Colloids Surf., B* **2012**, *97*, 211−220.
(175) Saldana, L.; et al. In Vitro Biocompatibility of an Ultra-fine-grained Zirconium. *Biomaterials* **2007**, *28*, 4343−4354.
(176) Lancaster, M. V.; Fields, R. D. *Antibiotic and Cytotoxic Drug Susceptibility Assays Using Resazurin and Poising Agents*. U.S. Patent No. US550195926 A, Mar. 26, 1996.
(177) Nie, F. L.; Wang, S. G.; Wang, Y. B.; Wei, S. C.; Zheng, Y. F. Comparative Study on Corrosion Resistance and In Vitro Biocompatibility of Bulk Nanocrystalline and Microcrystalline Biomedical 304 Stainless Steel. *Dent. Mater.* **2011**, *27*, 677−683.
(178) Misra, R. D. K.; Thein-Han, W. W.; Pesacreta, T. C.; Hasenstein, K. H.; Somani, M. C.; Karjalainen, L. P. Cellular Response of Preosteoblasts to Nanograined/Ultrafine-Grained Structures. *Acta Biomater.* **2009**, *5*, 1455−1467.
(179) Misra, R. D. K.; Thein-Han, W. W.; Pesacreta, T. C.; Hasenstein, K. H.; Somani, M. C.; Karjalainen, L. P. Favorable Modulation of Pre-osteoblast Response to Nanograined/Ultrafine-Grained Structures in Austenitic Stainless Steel. *Adv. Mater.* **2009**, *21*, 1280−1285.
(180) Misra, R. D. K.; Thein-Han, W. W.; Mali, S. A.; Somani, M. C.; Karjalainen, L. P. Cellular Activity of Bioactive Nanograined/Ultrafine-Grained Materials. *Acta Biomater.* **2010**, *6*, 2826−2835.
(181) Misra, R. D. K.; Thein-Han, W. W.; Somani, M. C.; Karjalainen, L. P. Phase Reversion-Induced Nanograined/Ultrafine-Grained Structures in Austenitic Stainless Steel and their Significance in Modulating Cellular Response: Biochemical and Morphological Study with Fibroblasts. *Adv. Eng. Mater.* **2009**, *11*, B235−B242.
(182) Misra, R. D. K.; Thein-Han, W. W.; Pesacreta, T. C.; Somani, M. C.; Karjalainen, L. P. Biological Significance of Nanograined/Ultrafine-Grained Structures: Interaction with Fibroblasts. *Acta Biomater.* **2010**, *6*, 3339−3348.
(183) Misra, R. D. K.; Nune, C.; Pesacreta, T. C.; Somani, M. C.; Karjalainen, L. P. Interplay Between Grain Structure and Protein Adsorption on Functional Response of Osteoblasts: Ultrafine-Grained versus Coarse-Grained Substrates. *J. Biomed. Mater. Res. Part A* **2013**, *101A*, 1−12.
(184) Misra, R. D. K.; Nune, C.; Pesacreta, T. C.; Somani, M. C.; Karjalainen, L. P. Understanding the Impact of Grain Structure in Austenitic Stainless Steel from a Nanograined Regime to a Coarse-Grained Regime on Osteoblast Functions Using a Novel Metal Deformation−Annealing Sequence. *Acta Biomater.* **2013**, *9*, 6245−6258.

(185) Faghihi, S.; Azari, F.; Zhilyaev, A.; Szpunar, J.; Vali, H.; Tabrizian, M. Cellular and Molecular Interactions between MC3T3-E1 Pre-osteoblasts and Nanostructured Titanium Produced by High-Pressure Torsion. *Biomaterials* **2007**, *28*, 3887−3895.
(186) Faghihi, S.; Zhilyaev, A. P.; Szpunar, J. A.; Azari, F.; Vali, H.; Tabrizian, M. Nanostructuring of a Titanium Material by High-Pressure Torsion Improves Pre-osteoblast Attachment. *Adv. Mater.* **2007**, *19*, 1069−1073.
(187) Nie, F. L.; Zheng, Y. F.; Cheng, Y.; Wei, S. C.; Valiev, R. Z. In Vitro Corrosion and Cytotoxicity on Microcrystalline, Nanocrystalline, and Amorphous NiTi Alloy Fabricated by High Pressure Torsion. *Mater. Lett.* **2010**, *64*, 983−986.
(188) Van Humbeeck, J. Non-medical Applications of Shape Memory Alloys. *Mater. Sci. Eng. A* **1999**, *273*, 134−148.
(189) Coogan, T. P.; Latta, D. M.; Snow, E. T.; Costa, M.; Lawrence, A. Toxicity and Carcinogenicity of Nickel Compounds. *Crit. Rev. Toxicol.* **1989**, *19*, 341−384.
(190) Keim, S.; Brunner, J. G.; Fabry, B.; Virtanen, S. Control of Magnesium Corrosion and Biocompatibility with Biomimetic Coatings. *J. Biomed. Mater. Res. B Appl. Biomater.* **2011**, *96B*, 84−90.
(191) Sunil, B. R.; Kumar, A. A.; Sampath Kumar, T. S.; Chakkingal, U. Role of Biomineralization on the Degradation of Fine Grained AZ31 Magnesium Alloy Processed by Groove Pressing. *Mater. Sci. Eng., C* **2013**, *33*, 1607−1615.
(192) Park, J. W.; Kim, Y. J.; Park, C. H.; Lee, D. H.; Ko, Y. G.; Jang, J. H.; Lee, C. S. Enhanced Osteoblast Response to an Equal Channel Angular Pressing-Processed Pure Titanium Substrate with Microrough Surface Topography. *Acta Biomater.* **2009**, *5*, 3272−3280.
(193) Cochran, D. L.; et al. The Use of Reduced Healing Times on ITI Implants with a Sandblasted and Acid-Etched (SLA) Surface. Clin. *Oral Implants Res.* **2002**, *13*, 144−153.
(194) Schneider, G. B.; Zaharias, R.; Seabold, D.; Keller, J.; Stanford, C. Differentiation of Preosteoblasts is Affected by Implant Surface Microtopographies. *J. Biomed. Mater. Res. Part A* **2004**, *69A*, 462−468.
(195) Gronthos, S.; Zannettino, A. C. W.; Graves, S. E.; Ohta, S.; Hay, S. J.; Simmons, P. J. Differential Cell Surface Expression of the STRO-1 and Alkaline Phosphatase Antigens on Discrete Developmental Stages in Primary Cultures of Human Bone Cells. *J. Bone Miner. Res.* **1999**, *14*, 47−56.
(196) Zhao, M.; et al. In Vitro Bioactivity and Biocompatibility Evaluation of Bulk Nanostructured Titanium in Osteoblast-like Cells by Quantitative Proteomic Analysis. *J. Mater. Chem. B* **2013**, *1*, 1926−1938.
(197) Nie, F. L.; et al. In Vitro and In Vivo Studies on Nanocrystalline Ti Fabricated by Equal Channel Angular Pressing with Microcrystalline CP Ti as Control. *J. Biomed. Mater. Res. Part A* **2013**, *101A*, 1694−1707.
(198) Zhao, C.; Ji, W.; Han, P.; Zhang, J.; Jiang, Y.; Zhang, X. In Vitro and In Vivo Mineralization and Osseointegration of Nanostructured Ti6Al4V. *J. Nanopart. Res.* **2010**, *13*, 645−654.
(199) Barrere, F.; Mahmood, T. A.; De Groot, K.; Van Blitterswijk, C. A. Advanced Biomaterials for Skeletal Tissue Regeneration: Instructive and Smart Functions. *Mater. Sci. Eng., R* **2008**, *59*, 38−71.
(200) Jiang, Y.; Jia, T.; Wooley, P. H.; Yang, S. Y. Current Research in the Pathogenesis of Aseptic Implant Loosening Associated with Particulate Wear Debris. *Acta Orthop. Belg.* **2013**, *79*, 1−9.
(201) Windler, M.; Klabunde, R.; Brunette, D. M. *Titanium in Medicine*; Springer Verlag: Berlin, 2001.
(202) Thompson, G. J.; Puleo, D. A. Ti-6Al-4V Ion Solution Inhibition of Osteogenic Cell Phenotype as a Function of Differentiation Timecourse In Vitro. *Biomaterials* **1996**, *17*, 1949−1954.
(203) Cadosch, D.; Chan, E.; Gautschi, O. P.; Filgueira, L. Metal is Not Inert: Role of Metal Ions Released by Biocorrosion in Aseptic Loosening Current Concepts. *J. Biomed. Mater. Res. Part A* **2009**, *91A*, 1252−1262.
(204) Sun, Z. L.; Wataha, J. C.; Hank, C. T. Effects of Metal Ions on Osteoblast-Like Cell Metabolism and Differentiation. *J. Biomed. Mater. Res.* **1997**, *34*, 29−37.
(205) Ko, Y. G.; Shin, D. H.; Park, K. T.; Lee, C. S. An Analysis of the Strain Hardening Behavior of Ultra-fine-grained Pure Titanium. *Scr. Mater.* **2006**, *54*, 1785−1789.
(206) Molina-Aldareguia, J. M.; Perez-Prado, M. T.; Valiev, R. Z.; Semenova, I. P.; Sabirov, I. High Strength Ultra-fine-grained Titanium Produced via a Novel SPD Processing Route. *Int. J. Mater. Form.* **2010**, *3*, 407−410.
(207) Eisenbarth, E.; et al. Interactions Between Cells and Titanium Surfaces. *Biomol. Eng.* **2002**, *19*, 243−249.
(208) Carbone, R.; et al. Biocompatibility of Cluster-Assembled Nanostructured TiO_2 with Primary and Cancer Cells. *Biomaterials* **2006**, *27*, 3221−3229.
(209) Ellingsen, J. E. A Study on the Mechanism of Protein Adsorption to TiO_2. *Biomaterials* **1991**, *12*, 593−596.
(210) Sousa, S. R.; Brás, M. M.; Moradas-Ferreira, P.; Barbosa, M. A. Dynamics of Fibronectin Adsorption on TiO2 Surfaces. *Langmuir.* **2007**, *23*, 7046−7054.
(211) Zhao, G.; Schwartz, Z.; Wieland, M.; Rupp, F.; Geis-Gerstorfer, J.; Cochran, D. L.; Boyan, B. D. High Surface Energy Enhances Cell Response to Titanium Substrate Microstructure. *J. Biomed. Mater. Res. Part A* **2005**, *74*, 49−58.
(212) Korotin, D. M.; Bartkowski, S.; Kurmaev, E. Z.; Neumann, M.; Yakushina, E. B.; Valiev, R. Z.; Cholakh, S. O. Surface Studies of Coarse-Grained and Nanostructured Titanium Implants. *J. Nanosci. Nanotechnol.* **2012**, *12*, 8567−8572.
(213) Sato, M.; Webster, T. J. Nanobiotechnology: Implications for the Future of Nanotechnology in Orthopedic Applications. *Expert Rev. Med. Devices.* **2004**, *1*, 105−114.
(214) García, A. J.; Vega, M. D.; Boettiger, D. Modulation of Cell Proliferation and Differentiation through Substrate-Dependent Changes in Fibronectin Conformation. *Mol. Biol. Cell.* **1999**, *10*, 785−798.
(215) Clem, W. C.; et al. Mesenchymal Stem Cell Interaction with Ultra-Smooth Nanostructured Diamond for Wear-Resistant Orthopaedic Implants. *Biomaterials* **2008**, *29*, 3461−3468.
(216) Denis, F. A.; Hanarp, P.; Sutherland, D. S.; Gold, J.; Mustin, C.; Rouxhet, P. G.; Dufrêne, Y. F. Protein Adsorption on Model Surfaces with Controlled Nanotopography and Chemistry. *Langmuir.* **2002**, *18*, 819−828.
(217) Steele, J. G.; McFarland, C.; Dalton, B. A.; Johnson, G.; Evans, M. D.; Howlett, C. R.; Underwood, P. A. Attachment of Human Bone Cells to Tissue Culture Polystyrene and to Unmodified Polystyrene: The Effect of Surface Chemistry upon Initial Cell Attachment. *J. Biomater. Sci. Polym. Ed.* **1993**, *5*, 245−257.
(218) Ivanov, A. E.; Ekeroth, J.; Nilsson, L.; Mattiasson, B.; Bergenståhl, B.; Galaev, I. Y. Variations of Wettability and Protein Adsorption on Solid Siliceous Carriers Grafted with Poly(N-isopropylacrylamide). *J. Colloid Interface Sci.* **2006**, *296*, 538−544.
(219) Boyan, B. D.; Hummert, T. W.; Dean, D. D.; Schwartz, Z. Role of Material Surfaces in Regulating Bone and Cartilage Cell Response. *Biomaterials* **1996**, *17*, 137−146.
(220) Klabunde, K. J.; et al. Nanocrystals as Stoichiometric Reagents with Unique Surface Chemistry. *J. Phys. Chem.* **1996**, *100*, 12142−12153.
(221) Tamayol, A.; Akbari, M.; Annabi, N.; Paul, A.; Khademhosseini, A.; Juncker, D. Fiber-Based Tissue Engineering: Progress, Challenges, and Opportunities. *Biotechnol. Adv.* **2013**, *31*, 669−687.
(222) Akbari, M.; Tamayol, A.; Laforte, V.; Annabi, N.; Hassani najafabadi, A.; Khademhosseini, A.; Juncker, D. Composite Living Fibers for Creating Tissue Constructs Using Textile Techniques. *Adv. Funct. Mater.* **2014**, DOI: 10.1002/adfm.201303655..
(223) Jayaraman, M.; Meyer, U.; Bühner, M.; Joos, U.; Wiesmann, H. P. Influence of Titanium Surfaces on Attachment of Osteoblast-like Cells In Vitro. *Biomaterials* **2004**, *25*, 625−631.
(224) Biela, S. A.; Su, Y.; Spatz, J. P.; Kemkemer, R. Different Sensitivity of Human Endothelial Cells, Smooth Muscle Cells, and Fibroblasts to Topography in the Nano−Micro Range. *Acta Biomater.* **2009**, *5*, 2460−2466.